Modeling the avoidance behavior of zooplankton on phytoplankton infected by free viruses

J Biol Phys manuscript No.
(will be inserted by the editor)

Saswati Biswas · Pankaj Kumar Tiwari · Francesca Bona · Samares Pal · Ezio Venturino

Modeling the avoidance behavior of zooplankton on phytoplankton infected by free viruses

the date of receipt and acceptance should be inserted later

Abstract In any ecosystem, chaotic situations may arise from equilibrium state for different reasons. To overcome these chaotic situations sometimes the system itself exhibits some mechanisms of self-adaptability. In this paper, we explore an eco-epidemiological model consisting of three aquatic groups: phytoplankton, zooplankton and marine free viruses. We assume that the phytoplankton population are infected by external free viruses and zooplankton get affected on consumption of infected phytoplankton; also the infected phytoplankton do not compete for resources with the susceptible one. In addition, we model a mechanism by which zooplankton recognize and avoid infected phytoplankton, at least when susceptible phytoplankton are present. The zooplankton extinction chance increases on increasing the force of infection or decreasing the intensity of avoidance. Further, when the viral infection triggers chaotic dynamics, high zooplankton avoidance intensity can stabilize again the system. Interestingly, for high avoidance intensity, nutrient enrichment has a destabilizing effect on the system dynamics, which is in line with the *paradox of enrichment*. Global sensitivity analysis helps to identify the most significant parameters that reduce the infected phytoplankton in the system. Finally, we

Saswati Biswas · Pankaj Kumar Tiwari · Samares Pal
Department of Mathematics, University of Kalyani, Kalyani - 741235, India

Francesca Bona
DBIOS, University of Turin, via Accademia Albertina 13, 10123 Turin, Italy

Ezio Venturino
Dipartimento di Matematica "Giuseppe Peano", via Carlo Alberto 10, 10123 Torino, Università di Torino, Italy; Member of the INdAM research group GNCS
E-mail: ezio.venturino@unito.it

compare the dynamics of the system by allowing the infected phytoplankton also to share resources with the susceptible phytoplankton. A gradual increase of the virus replication factor turns the system dynamics from chaos to doubling state to limit cycle to stable and the system finally settles down to the zooplankton-free equilibrium point. Moreover, on increasing the intensity of avoidance, the system shows a transcritical bifurcation from the zooplankton-free equilibrium to the coexistence steady state, and remains stable thereafter.

Keywords Phytoplankton · Zooplankton · Free-virus · Avoidance behavior · Chaos · Global sensitivity.

1 Introduction

Phytoplankton lie at the bottom of the aquatic trophic chains. Due to presence of chlorophyll pigment in the cells, phytoplankton grow photoautotrophically in aquatic environments [1]. These unicellular organisms are basically the energy sources, from which energy flows along the food webs up to the higher trophic levels. Any potential changes in these primary producers can therefore affect the entire food chain structure. Marine viruses have been recognized to play a major role in altering the metabolic capacity as well as the biochemical compositions of their algal hosts [2–6]. Moreover, many studies have illustrated the ecological importance of marine viruses as agents causing mortality in marine phytoplankton communities [7–11]. In the last few decades, worldwide attention has been drawn towards the impacts of diseases in ecological systems [12, 13]; in particular, algal-virus correlations and their effects on interspecies competition as well as on environmental issues [14, 15].

Marine viruses are exceptionally abundant, highly host-specific and have the feature of possibly infect the algae. There are two predominant ways for viral replication: the lytic and lysogenic cycle. Most of the non-enveloped and few enveloped marine viruses replicate through lytic cycles. Namely, virus particles get attached to their algal host cells and inject genome into the cell. Virus replication is performed using the hosts genetic machinery. After the completion of replication, the cell wall breaks and progeny virions are released into the environment. Viral infection alters the size, nutritional value and cell lipid membrane characteristics of the host cells. It also directly impacts on the grazing behavior and growth rate of zooplankton [16, 17]. The coccolithophores *Emiliania huxleyi* are frequently found to be one of the dominant phytoplankton species in many pelagic ecosystems. In favourable water conditions, *E. huxleyi* can grow extremely rapidly and it forms very extensive blooms especially at high latitude [18]. It is well documented that *E. huxleyi* blooms are exterminated by viral lysis, with the

viruses unambiguously identified as EhV [19]. During viral infection *E. huxleyi* experiences remarkable structural, biochemical and physiological changes [5, 20, 21], which in turn affect the herbivory grazing.

In the normal bloom conditions when viral infection has not yet started, the primary consumers like copepods, randomly feed on *E. huxleyi* and other phytoplankton species. In the presence of viral infection, however, zooplankton exhibit some grazing selection. Some zooplankton (e.g. *Acartia tonsa*) tend to avoid infected *E. huxleyi* cells in response to the chemicals released by the infected cell through their surface [18, 20]. Under stress (i.e., in the presence of grazers) algal cells liberate a moderate amount of chemicals such as dimethyl sulfide (DMS) and amino acids [22–25], which give signals to their grazers. Feeding on them will be poisonous to the grazers, so they prefer to avoid them. But during viral infection the DMS release increases considerably and becomes toxic [26, 27]. In such conditions, *Acartia tonsa* preferably ingests less infected than uninfected *E. huxleyi* cells. A further effect of consumed high lyase *E. huxleyi* cells is the increase of zooplankton mortality, caused by the reaction of the produced dimethyl gas and of the *E. huxleyi's* calcium carbonate cell with the zooplankton's internal pH, with the consequent destruction of the latter [28].

Predator-prey systems with viral infection affecting the prey have been considered in [29–32], while the role of viral infection in the marine trophic chains has been investigated more specifically in [33–36]. In [37] viral infection as a cause of recurrent phytoplankton blooms has been analyzed by formulating a three-species model consisting of susceptible and infected phytoplankton and their potential grazer. A virally infected phytoplankton-zooplankton system considering both susceptible and infected phytoplankton being able to release toxic substances appears in [38]. The viral infection and "allelopathic agents" are shown to possess a major role for the control of phytoplankton blooms. The dynamics of ecological interactions caused by the infected phytoplankton where the disease is transmitted through contact have been investigated for instance in [39–42], while other models have been formulated to take into account that the disease is transmitted also through vectors or directly from the environment, e.g., pollutants, toxicant, free viruses etc., [14, 15], with the typical assumption that both the healthy and infected phytoplankton are equally likely to predation and infected phytoplankton has no negative impact on the growth of zooplankton.

Ecological systems possess all the elements to produce chaotic dynamics [43]. Although chaos is commonly predicted by mathematical models, evidence for its existence in the natural world is scarce and inconclusive. Even the characteristics of chaos and its presence in nature are much discussed in ecology [44–47]. Recent developments in dynamical system theory consider chaotic fluctuations of a

dynamical system as highly desirable because fluctuations allow such a system to be easily controlled. To assess the ecological implications of chaotic dynamics in different natural systems, it is important to explore changes in the dynamics when structural assumptions of the system are varied. One approach to the study of the dynamics of ecological community is via its food web and the coupling of interacting species with each other. Hastings and Powell [48] produced chaos in a three species food chain model with Holling type II functional responses. Chattopadhyay and Sarkar [49] modified the Hastings and Powell [48] model by introducing toxin producing parameter and its negative effect on zooplankton grazing on phytoplankton. Jørgensen [47] showed that chaos may appear in the planktonic system due to size variation in zooplankton species. According to the allometric principle of Peters [50], all the parameters vary as functions of size. Mandal et al. [51] applied thermodynamic principle (exergy) in the Hastings and Powell's model of phytoplankton, zooplankton and fish, showing that on gradually decreasing the zooplankton size the model dynamics changes from an equilibrium state to chaotic conditions.

In the present investigation, the key contribution is represented by the modeling of grazer zooplankton avoidance of virally infected phytoplankton in the presence of susceptible phytoplankton [17]. The variation in the zooplankton's avoidance degree of infected phytoplankton when the susceptible phytoplankton levels change may have a relevant impact for the species survival and for the understanding of the internal system dynamics. The previous related model of [52] dealing with the avoidance phenomenon in the presence of toxic phytoplankton, showed that the strength of avoidance deeply influences the dominance of the toxic species. In contrast to the other former studies [14,15], a negative effect of infected cell consumption on zooplankton, arising from the toxic chemical compounds released by viral cell lysis [17,28], is incorporated in the present model. We study the system dynamics in two cases: at first we assume that the infected phytoplankton do not compete with susceptible phytoplankton for resources, while in the second case, the resources are assumed to be shared by susceptible and infected phytoplankton. The model contains the zooplankton feeding avoidance of infected phytoplankton as a function of the abundance of susceptible phytoplankton. Our objective is to assess whether the avoidance behavior enhances the survival and dominance of infected phytoplankton over its susceptible competitors, as well as its effect on the zooplankton. In chaotic situations, the negative effect of infected phytoplankton on zooplankton may reduce the grazing pressure of zooplankton and as a result the system may recover from chaos and return to a stable state.

The rest of the paper is organized as follows: in the next section, we formulate the mathematical model incorporating the zooplankton avoidance of infected phytoplankton in the presence of the susceptible one. The mathematical analysis in Section 3 contains the analytical findings of the model; Hopf-bifurcation analysis is performed by taking the avoidance intensity as bifurcation parameter. In Section 4, we numerically investigate the dynamical behavior of the system for the different parameters setups. In so doing we validate the criteria obtained from the mathematical analysis illustrated in Section 3. This section also contains the investigation of the system behavior when susceptible and infected phytoplankton compete for common resources. A final discussion concludes the paper.

2 The mathematical model

Viruses represent the most abundant entities in the sea and play a major role in the control of oceans life. However, not much is known about marine viruses and their ecological role in aquatic ecosystems, their interaction with other species, the spread of diseases and their impact on plankton blooming. We consider an ecological system consisting of susceptible phytoplankton (S), infected phytoplankton (I), zooplankton (Z) and the free viruses in the environment causing the infection (V) under the following assumptions:

1. In the absence of viral disease and the grazer zooplankton, the susceptible phytoplankton grow logistically with intrinsic growth rate a and carrying capacity K.
2. The susceptible phytoplankton S, becomes infected by direct contact with free viruses, V. This is modeled via the function
$$T_0(S,V) = \frac{\beta SV}{K_1 + V}$$
with transmission rate β and half saturation constant K_1 [14].
3. Zooplankton predate on both susceptible and infected phytoplankton; while they benefit the grazing of the former [14,15], uptake of infected phytoplankton instead inhibits them [17,26,27].
4. The Holling type-II functional response to the grazer zooplankton is assumed for susceptible and infected phytoplankton respectively given by
$$f_S = \frac{\alpha_1 SZ}{d_1 + S}, \quad f_I = \frac{\alpha_2 IZ}{d_2 + I},$$
where d_1 and d_2 denote the half-saturation constants for the susceptible and infected phytoplankton.
5. Several experimental outcomes reveal that whenever abundance of susceptible phytoplankton is high, zooplankton prefer to graze on susceptible phytoplankton and avoid ingesting infected species

[17]. Also, zooplankton graze on infected phytoplankton in the presence of susceptible phytoplankton. Moreover, infected phytoplankton has no significant influence on the predation of susceptible phytoplankton, but the abundance of susceptible phytoplankton greatly reduces the ingestion of infected phytoplankton.

6. To account for the fact that the presence of susceptible phytoplankton abundance greatly reduces the ingestion of infected phytoplankton, we modify the predation rate on infected phytoplankton by introducing an extra term γS in the denominator of the relevant functional response as [52],

$$f_I^* = \frac{\alpha_2 IZ}{d_2 + I + \gamma S},$$

where γ measures the intensity of the avoidance of infected phytoplankton by zooplankton in the presence of susceptible phytoplankton.

7. $\gamma = 0$ produces a system where zooplankton do not discriminate between susceptible and infected phytoplankton; whereas high γ results in a decrease in the uptake of infected phytoplankton by zooplankton in the presence of susceptible phytoplankton, although it does not affect the uptake of susceptible phytoplankton directly. Thus, higher values of γ result in the lesser mortality of the zooplankton due to ingestion of infected phytoplankton. Zooplankton natural mortality is taken as a linear function, νZ.
8. The infected phytoplankton fail to contribute in the reproduction process due to their inability to compete for resources [53,54] as the energy required for viral replication of infected phytoplankton is negligible, and they are removed by cell lysis before having the capability of reproducing [55, 56]. Further, the infected phytoplankton are assumed not to exert intraspecific pressure on the susceptible phytoplankton [37].
9. From the time of infection to its lysis, within the body of the infected phytoplankton viruses replicate. Let μ represent the infected phytoplankton mortality rate and $b \gg 1$ the virus replication factor, i.e., the average number of viruses released in the environment upon infected phytoplankton lysis. The decay rate of virus is assumed to be constant, δ. The virus is removed through the infection of susceptible phytoplankton at the rate $T_0(S, V)$.

Based on the above assumptions, the schematic diagram for the interactions among susceptible phytoplankton, infected phytoplankton, zooplankton and free viruses is depicted in Fig. 1. Thus, we obtain

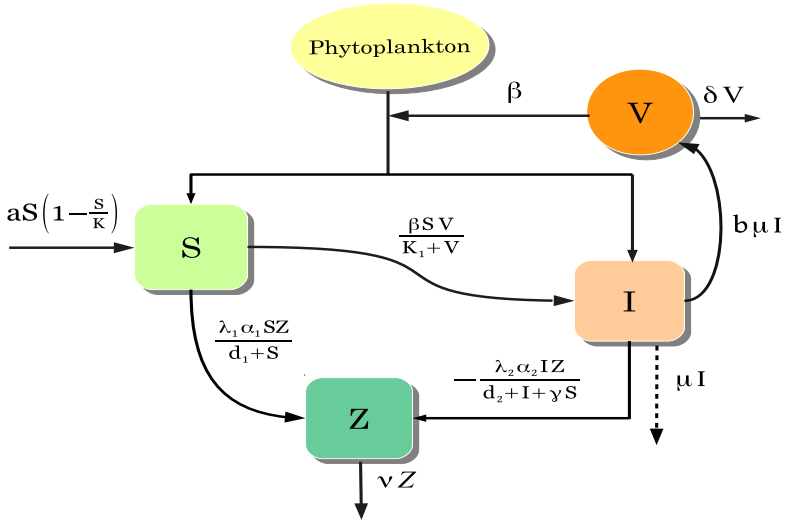

Fig. 1 Schematic diagram of system (1).

the following system of differential equations,

$$\begin{aligned}
\frac{dS}{dt} &= aS\left(1-\frac{S}{K}\right)-\frac{\alpha_1 SZ}{d_1+S}-\frac{\beta SV}{K_1+V},\\
\frac{dI}{dt} &= \frac{\beta SV}{K_1+V}-\frac{\alpha_2 IZ}{d_2+I+\gamma S}-\mu I,\\
\frac{dZ}{dt} &= \frac{\lambda_1\alpha_1 SZ}{d_1+S}-\frac{\lambda_2\alpha_2 IZ}{d_2+I+\gamma S}-\nu Z,\\
\frac{dV}{dt} &= b\mu I-\frac{\beta SV}{K_1+V}-\delta V.
\end{aligned} \tag{1}$$

All parameters involved in the system (1) are assumed to be positive, and their biological meanings are given in Table 1.

3 Mathematical Analysis

We first have the following theorem regarding the positivity property, boundedness and permanence of the system (1).

Theorem 1 *System (1) is positively invariant and bounded in R^4_+, and the feasible region for system (1) is the following set*

$$\Omega=\left\{(S,I,Z,V):\ 0\le S+I+Z+\frac{\nu}{b\mu}V\le M\right\},$$

Table 1 The meaning of the model parameters and their hypothetical values, chosen within ranges prescribed in the literature [14,15].

Parameters	Descriptions	Values	Units
a	Intrinsic growth rate of susceptible phytoplankton	0.75	day^{-1}
K	Carrying capacity of susceptible phytoplankton	108	cells L^{-1}
α_1	Consumption rate of susceptible phytoplankton by zooplankton	0.045	day^{-1}
d_1	Half-saturation constant for the consumption of susceptible phytoplankton by zooplankton	2	cells L^{-1}
β	Force of infection	0.65	day^{-1}
K_1	Half-saturation constant for the infection of susceptible phytoplankton by free-viruses	3	cells L^{-1}
α_2	Consumption rate of infected phytoplankton by zooplankton	0.045	day^{-1}
d_2	Saturation constant for the consumption of infected phytoplankton by zooplankton	2	cells L^{-1}
γ	Intensity of avoidance	3.8	—
μ	Death rate of infected phytoplankton	0.16	day^{-1}
λ_1	Growth of zooplankton on consumption of susceptible phytoplankton	0.75	—
λ_2	Death of zooplankton on consumption of infected phytoplankton	0.61	—
ν	Death rate of zooplankton	0.012	day^{-1}
b	Virus replication factor	35	—
δ	Decay rate of free viruses	1.23	day^{-1}

which is compact and invariant with respect to system (1). Further, let the following inequalities be satisfied, where S_a, I_m, Z_m and V_m are defined in the proof:

$$a > \frac{\beta V_m}{K_1} + \frac{\alpha_1 Z_m}{d_1},\ \beta > \frac{I_m}{S_a}\left(\frac{\alpha_2 Z_m}{d_2} + \mu\right),\ \frac{\lambda_1\alpha_1 S_a}{d_1 + S_a} > \nu + \frac{\lambda_2\alpha_2 I_m}{d_2}. \tag{2}$$

Then the system (1) is uniformly persistent.

Proof System (1) has a Lipschitz-continuous right hand side, so that the existence and uniqueness theorem for its solutions holds. Observe further that it is homogeneous, so that the coordinate axes and (hyper)planes cannot be crossed, being themselves solutions. Therefore, any trajectory of the system (1) starting from an initial state in $\mathbb{R}^4_+$ remains trapped in $\mathbb{R}^4_+$.

We define a new variable $U = S + I + Z + \frac{\nu}{b\mu}V$. For an arbitrary $\sigma > 0$, by summing up the equations in system (1), we find

$$\frac{dU}{dt} + \sigma U = (a+\sigma)S - \frac{aS^2}{K} - \{(\mu-\nu)-\sigma\}I - (\nu-\sigma)Z - \frac{\nu}{b\mu}(\delta-\sigma)V - \frac{(1-\lambda_1)\alpha_1 SZ}{d_1+S} - \frac{(1+\lambda_2)\alpha_2 IZ}{d_2+I+\gamma S} - \frac{\nu}{b\mu}\frac{\beta SV}{K_1+V}.$$

Since $\lambda_1 \leq 1$, after choosing $\sigma \leq \min\{(\mu-\nu), \nu, \delta\}$, we obtain the following upper bound:

$$\frac{dU}{dt} + \sigma U \leq (a+\sigma)S - \frac{aS^2}{K} \leq \frac{K(a+\sigma)^2}{4a} = L.$$

Applying standard results on differential inequalities [57], we have

$$U(t) \leq e^{-\sigma t}\left(U(0) - \frac{L}{\sigma}\right) + \frac{L}{\sigma} \leq \max\left\{\frac{L}{\sigma}, U(0)\right\} = M.$$

Thus, there exists an $M > 0$, depending only on the system parameters, such that $U(t) \leq M$. Hence, the solutions of system (1) and consequently all the system populations are ultimately bounded above.

Since

$$\limsup_{t\to\infty}\left[S(t) + I(t) + Z(t) + \frac{\nu}{b\mu}V(t)\right] \leq M$$

and $\lim_{t\to\infty} S(t) \leq K$, there exist T_1, T_2, T_3, $T_4 > 0$ such that $S(t) \leq K \ \forall\ t \geq T_1$, $I(t) \leq I_m \ \forall\ t \geq T_2$, $Z(t) \leq Z_m \ \forall\ t \geq T_3$, $V(t) \leq V_m$ for all $t \geq T_4$, where I_m, Z_m and V_m are finite positive constants with $K + I_m + Z_m + V_m \leq M$. Hence, for all $t \geq \max\{T_1, T_2, T_3, T_4\} = T$, $S(t) \leq K$, $I(t) \leq I_m$, $Z(t) \leq Z_m$ and $V(t) \leq V_m$. Let us define $M_1 = \max\{K, I_m, Z_m, V_m\}$.

Now, from the first equation of system (1), we have

$$\frac{dS}{dt} \geq aS\left(1 - \frac{S}{K}\right) - \frac{\beta S V_m}{K_1} - \frac{\alpha_1 S Z_m}{d_1}.$$

Hence, it follows that for some S_a,

$$\liminf_{t\to\infty} S(t) \geq \frac{K}{a}\left(a - \frac{\beta V_m}{K_1} - \frac{\alpha_1 Z_m}{d_1}\right) = S_a.$$

From the second equation of system (1), we have

$$\frac{dI}{dt} \geq \frac{\beta S_a V}{K_1 + V} - \frac{\alpha_2 Z_m I_m}{d_2} - \mu I_m > 0$$

provided that

$$V(t) > \frac{K_1 I_m\left(\frac{\alpha_2 Z_m}{d_2} + \mu\right)}{\beta S_a - I_m\left(\frac{\alpha_2 Z_m}{d_2} + \mu\right)}.$$

Let $V_a > 0$ be such that

$$\frac{K_1 I_m\left(\frac{\alpha_2 Z_m}{d_2} + \mu\right)}{\beta S_a - I_m\left(\frac{\alpha_2 Z_m}{d_2} + \mu\right)} < V_a < V_m,$$

then $\frac{dI}{dt} > 0$ for $V(t) \geq V_a > 0$, for all $t > T$. So, there exist $T_5 > 0$ and $0 < I_a < I_m$ such that $I(t) \geq I_a$ for all $t \geq T_5$. Therefore, for all $t \geq \max\{T, T_5\} = T'$ if $V_a \leq V(t) \leq V_m$, then $I_a \leq I(t) \leq I_m$.

From the third equation of system (1), we have

$$\frac{dZ}{dt} \geq Z\left(\frac{\lambda_1\alpha_1 S_a}{d_1+S_a} - \frac{\lambda_2\alpha_2 I_m}{d_2} - \nu\right).$$

Hence, it follows that for some Z_a,

$$\lim_{t\to\infty} \inf Z(t) \geq Z(0) = Z_a$$

provided that

$$\frac{\lambda_1\alpha_1 S_a}{d_1+S_a} > \nu + \frac{\lambda_2\alpha_2 I_m}{d_2}.$$

Let $M_2 = \min\{S_a, I_a, Z_a, V_a\}$. For M_2 to be positive, conditions in (2) must hold. Hence, the theorem follows.

3.1 The ecosystem in the absence of free-viruses

In the absence of viral disease in phytoplankton, system (1) reduces to the following simple subsystem,

$$\begin{aligned}\frac{dS}{dt} &= aS\left(1-\frac{S}{K}\right) - \frac{\alpha_1 SZ}{d_1+S},\\ \frac{dZ}{dt} &= \frac{\lambda_1\alpha_1 SZ}{d_1+S} - \nu Z,\end{aligned} \tag{3}$$

whose dynamics have been well studied [58]. Here, we summarize its dynamics as follows. System (3) has three feasible equilibria.

1. The plankton-free equilibrium $e_0 = (0,0)$, which is always a saddle.
2. If $K(\lambda_1\alpha_1 - \nu) < d_1\nu$, then the zooplankton-free equilibrium $e_1 = (K,0)$ is globally asymptotically stable.
3. If $K(\lambda_1\alpha_1 - \nu) > d_1\nu$ and $K < \dfrac{d_1(\lambda_1\alpha_1+\nu)}{\lambda_1\alpha_1-\nu}$, then the coexistence equilibrium $e_* = (S_*, Z_*)$ is globally asymptotically stable, where

$$S_* = \frac{d_1\nu}{\lambda_1\alpha_1-\nu},\ Z_* = \frac{\lambda_1 a d_1\{K(\lambda_1\alpha_1-\nu)-d_1\nu\}}{K(\lambda_1\alpha_1-\nu)^2}.$$

4. If $K(\lambda_1\alpha_1 - \nu) > d_1\nu$ and $K > \dfrac{d_1(\lambda_1\alpha_1+\nu)}{\lambda_1\alpha_1-\nu}$, then there is a unique globally asymptotically stable limit cycle around the coexistence equilibrium $e_* = (S_*, Z_*)$.

3.2 Equilibrium analysis of full system (1)

System (1) exhibits five non-negative equilibria, of which the origin $E_0 = (0, 0, 0, 0)$ and the point with only susceptible phytoplankton $E_1 = (K, 0, 0, 0)$ are always feasible. The disease-free equilibrium $E_2 = (S_2, 0, Z_2, 0)$, with

$$S_2 = \frac{\nu d_1}{\lambda_1\alpha_1 - \nu}, \quad Z_2 = \frac{K(\lambda_1\alpha_1 - \nu) - \nu d_1}{K(\lambda_1\alpha_1 - \nu)}$$

is feasible provided the following inequality holds

$$K(\lambda_1\alpha_1 - \nu) - \nu d_1 > 0. \tag{4}$$

The zooplankton-free equilibrium $E_3 = (S_3, I_3, 0, V_3)$ has the populations

$$S_3 = \frac{K\{aK_1 + V_3(a-\beta)\}}{a(K_1 + V_3)}, \quad I_3 = \frac{K\beta V_3\{aK_1 + V_3(a-\beta)\}}{a\mu(K_1 + V_3)^2},$$

where V_3 is a positive root of the quadratic

$$a_2V^2 + a_1V + a_0 = 0, \tag{5}$$

with coefficients

$$a_2 = a\delta, \quad a_1 = 2aK_1\delta - (b-1)\beta K(a-\beta), \quad a_0 = aK_1[\delta K_1 - \beta K(b-1)].$$

A necessary condition for feasibility is then $S_3 \geq 0$, which entails

$$aK_1 + V_3(a-\beta) > 0. \tag{6}$$

Because $a_2 > 0$, equation (5) has exactly one positive root if $a_0 < 0$. Thus, sufficient conditions for E_3 to be feasible are given by

$$aK_1 + V_3(a-\beta) > 0, \quad \beta K(b-1) - \delta K_1 > 0. \tag{7}$$

In case the latter is not satisfied, equation (5) has either two or no positive roots.

Coexistence $E^* = (S^*, I^*, Z^*, V^*)$ can be completely characterized. It has the populations:

$$Z^* = \frac{d_1 + S^*}{\alpha_1}\left[a\left(1 - \frac{S^*}{K}\right) - \frac{\beta V^*}{K_1 + V^*}\right], \quad I^* = F_1(S^*), \quad V^* = \frac{K_1F_2(S^*)}{\beta - F_2(S^*)}, \tag{8}$$

where

$$F_1(S) = \frac{(d_2 + \gamma S)[\nu(d_1 + S) - \lambda_1\alpha_1 S]}{\lambda_1\alpha_1 S - (d_1 + S)(\lambda_2\alpha_2 + \nu)} = \gamma C\frac{(S - S^-_{F_1})(S^0_{F_1} - S)}{S - S^\infty_{F_1}},\ C = \frac{\alpha_1\lambda_1 - \nu}{\alpha_1\lambda_1 - \alpha_2\lambda_2 - \nu}, \tag{9}$$

$$S^0_{F_1} = \frac{\nu d_1}{\alpha_1\lambda_1 - \nu}, \quad S^-_{F_1} = -\frac{d_2}{\gamma} < 0, \quad S^\infty_{F_1} = \frac{d_1(\alpha_2\lambda_2 + \nu)}{\alpha_1\lambda_1 - \alpha_2\lambda_2 - \nu}, \tag{10}$$

$$F_2(S) = \frac{\nu(d_1 + S) - \lambda_1\alpha_1 S}{\nu(d_1 + S) - (\lambda_1 + \lambda_2)\alpha_1 S}\left[a\left(1 - \frac{S}{K}\right) - \frac{\mu\alpha_1\lambda_2(d_2 + \gamma S)}{\lambda_1\alpha_1 S - (d_1 + S)(\lambda_2\alpha_2 + \nu)}\right] \tag{11}$$

and S^* is positive root of the equation

$$F_1(S) = \Phi(S), \quad \Phi(S) = \frac{1}{b\mu} F_2(S) \left[S + \delta \frac{K_1}{\beta - F_2(S)} \right]. \tag{12}$$

Analyzing the coefficients in F_1, by taking

$$\alpha_1 \lambda_1 \geq \alpha_2 \lambda_2 + \nu \tag{13}$$

it follows that $C > 0$ and then $0 \leq S^0_{F_1} \leq S^\infty_{F_1}$. Indeed the opposite case in (13) leads to $F_1(S) < 0$ for $S \geq 0$, which is not feasible. Further, the case $S^0_{F_1} \leq 0 \leq S^\infty_{F_1}$ is impossible, giving a contradiction on the signs of the coefficients of F_1. Finally, $F_1(S) \geq 0$ for $I_{F_1>0} = S^0_{F_1} \leq S < S^\infty_{F_1}$, which is the only range of interest where to seek a solution of (12) in what follows.

We now perform the qualitative study of $\Phi(S)$ in steps. As mentioned above, we concentrate on the interval $I_{F_1>0}$ in which F_1 is feasible, because the solution of the intersection problem (12) must be feasible, and therefore lie in this range.

First of all, we concentrate on $F_2(S)$. This function can be rewritten as follows:

$$F_2(S) = \frac{C}{S^\infty_{F_2} - S} \left[a(S^0_{F_1} - S) \left(1 - \frac{S}{K} \right) - \mu\alpha_1\lambda_2 F_1(S) \right] = C \frac{S^0_{F_1} - S}{(S^\infty_{F_2} - S)(S - S^\infty_{F_1})} \Psi(S),$$

$$S^\infty_{F_2} = \frac{\nu d_1}{\alpha_1(\lambda_1 + \lambda_2) - \nu}, \quad \Psi(S) = a \left(1 - \frac{S}{K} \right) (S - S^\infty_{F_1}) - \mu\alpha_1\lambda_2 (S - S^-_{F_1}) = \sum_{k=0}^{2} \theta_k S^k,$$

$$\theta_2 = -\frac{a}{K} < 0, \quad \theta_1 = a \left(\frac{S^\infty_{F_1}}{K} + 1 \right) - \mu\alpha_1\lambda_2, \quad \theta_0 = -aS^\infty_{F_1} + \mu\alpha_1\lambda_2 S^-_{F_1} < 0.$$

Thus, note that in view of (13) and (9), $0 < S^\infty_{F_2} \leq S^0_{F_1}$. Also $F_2(S^0_{F_1}) = 0$, the same zero as for $F_1(S)$.

The parabola Ψ is concave and it may or may not have real roots $\Psi^\pm$ depending on the sign of its discriminant $\Delta_\Psi = \theta_1^2 - 4\theta_0\theta_2$. If $\Delta_\Psi < 0$, it follows $\Psi(S) < 0$ for every $S \in \mathbf{R}$ and consequently $F_2(S) < 0$. This situation is illustrated in case (Z1) below. In case the real roots $\Psi^\pm$ exist, there are several subcases that need to be analysed based on their location on the real axis with respect to the three relevant fixed knots, arranged, as we know, in the following order $0 < S^\infty_{F_2} < S^0_{F_1} < S^\infty_{F_1}$. To study these various situations, the signs of $S - S^\infty_{F_1}$, $S^0_{F_1} - S$ and $S^\infty_{F_2} - S$ need to be considered. In the interval $I_{F_1>0}$, we find $S - S^\infty_{F_1} < 0$, $S^0_{F_1} - S < 0$ and $S^\infty_{F_2} - S < 0$. By coupling them with the study of F_2, we find the following results.

(Z1) Here $\Delta_\Psi < 0$ and $\Psi(S) < 0$, so that $F_2(S) > 0$ for every $S \in I_{F_1>0}$.

(Z2) $\Delta_\Psi > 0$; $\Psi^\pm$ lie both to the left or both to the right of $I_{F_1>0}$. Then $F_2(S) > 0$ for every $S \in I_{F_1>0}$.

(Z3) $\Delta_\Psi > 0$; if $S^0_{F_1} < \Psi^- < \Psi^+ < S^\infty_{F_1}$, then $F_2(S) > 0$ for $S^0_{F_1} < S < \Psi^-$ and for $\Psi^+ < S < S^\infty_{F_1}$.

(Z4) $\Delta_\Psi > 0$; if $\Psi^- < S^0_{F_1} < \Psi^+ < S^\infty_{F_1}$, then $F_2(S) > 0$ for $\Psi^+ < S < S^\infty_{F_1}$.

(Z5) $\Delta_\Psi > 0$; if $S^0_{F_1} < \Psi^- < S^\infty_{F_1} < \Psi^+$, then $F_2(S) > 0$ for $S^0_{F_1} < S < \Psi^-$.

(Z6) $\Delta_\Psi > 0$; if $\Psi^- < S^0_{F_1} < S^\infty_{F_1} < \Psi^+$, then $F_2(S) < 0$ for every $S \in I_{F_1>0}$ and consequently from (12) also $\Phi(S) < 0$ so that no feasible intersection can exist.

We now examine the possibility of solving (12) in the feasible range $I_{F_1>0}$, for each case. Note that F_2 has the same zero $S^0_{F_1}$ of F_1 and contains in its definition the latter function, so that it inherits its vertical asymptote too, $S^\infty_{F_1}$.

(Z1)–(Z2) In this situation $F_2(S) > 0$ for every $S \in I_{F_1>0}$. In view of the above remarks, its graph must raise up from $(S^0_{F_1}, 0)$ to infinity as S approaches from the left $S^\infty_{F_1}$. Note then that $Y = \beta$ always intersects the graph of F_2. We now construct the function Φ in steps. The function $\widetilde{\Pi}(S) = \beta - F_2(S)$ is positive for $S^0_{F_1} < S \leq A^+$ where it is zero. Then $\widetilde{\Pi}(S) = [\widehat{\Pi}(S)]^{-1}$ is positive in the same interval, but has a vertical asymptote at $S = A^+$ and negative in $(A^+, S^\infty_{F_1}]$, at which point it has a zero. Thus $\Pi(S) = S + \widehat{\Pi}(S)$ is nonnegative in $\{[S^0_{F_1}, A^+]\} \cup \{[\Pi^+, S^\infty_{F_1}]\}$ where Π^+ denotes a zero of $\Pi(S)$. Finally $\Phi(S) = (b\mu)^{-1} F_2(S)\Pi(S)$ has zeros at $S^0_{F_1}$ and Π^+ and from each one of these points on the S axis, a branch emanates raising up to infinity, the former (i) at A^+ and the second one (ii) at $S^\infty_{F_1}$. Comparing this behavior with the one of $F_1(S)$ described formerly, the intersection with the branch (ii) may not always exists, as the F_2 and F_1 are asymptotic to each other; indeed they have the same vertical asymptote there. Another one might occur with branch (i), if the following sufficient condition on the slopes of the two functions is guaranteed, so that the functions interlace, namely

$$F_1'(S^0_{F_1}) > \Phi'(S^0_{F_1}). \tag{14}$$

(Z3) This case gives rise to two subcases, as F_2 has one positive hump connecting the points $(S^0_{F_1}, 0)$ and $(\Psi^-, 0)$ and the branch tending to the vertical asymptote at $S^\infty_{F_1}$ from $(\Psi^+, 0)$, depending on whether $Y = \beta$ intersects or not the hump of F_2.

(Z3a) $Y = \beta$ has three intersections with F_2, with abscissae A^-, A^0, A^+. Then $\widetilde{\Pi}(S) = \beta - F_2(S)$ has zeros at these points and is positive in $[S^0_{F_1}, A^-]$ and in $[A^0, A^+]$. Both $\widehat{\Pi}(S)$ and $\Pi(S)$ have asymptotes at A^-, A^0 and A^+, as well as the resulting $\Phi(S)$, which is nonnegative in each one of the following intervals: $[S^0_{F_1}, A^-]$, $[A^0, \Pi^-]$, $[\Pi^+, A^+]$, $[A^*, S^\infty_{F_1})$. Thus Φ has four branches that either raise up to or come down from infinity and join the points on the S axis with abscissae $S^0_{F_1}$, Π^-, Π^+, A^*. Thus F_1 is bound to intersect the two intermediate of them, is asympototic to the rightmost one, and might intersect the leftmost one if the condition (14) holds.

(Z3b) In this subcase only one intersection of $Y = \beta$ with F_2 exists, giving rise to the zero A^+ of $\widetilde{\Pi}$. The latter function is positive for $S^0_{F_1} \leq S \leq S^+$, $\widehat{\Pi}$, Π and Φ possess a vertical asymptote at $S = A^+$. Thus Π is nonnegative in the intervals $[S^0_{F_1}, A^-]$, $[A^0, \Pi^-]$, $[\Pi^+, A^+)$, $[A^*, S^\infty_{F_1})$. Comparing with F_1 an intersection occurs with the branch lying in $[\Pi^+, A^+)$ and a second one might occur in the first interval $[S^0_{F_1}, A^-]$ if the slope of F_1 in this case is small enough, precisely if

$$F_1'(S^0_{F_1}) < \Phi'(S^0_{F_1}). \tag{15}$$

(Z4) The function F_2 is intercepted by $Y = \beta$ only once, as it possesses only one nonnegative branch in $[\Psi^+, S^\infty_{F_1})$. It follows that $\widetilde{\Pi}$ is nonnegative in $[S^0_{F_1}, A^+]$, $\widehat{\Pi}$ is also, but has a vertical asymptote at $S = A^+$, the same occurs for Π, which is nonnegative also in $[\Pi^+, S^\infty_{F_1})$. As a consequence, Φ has two branches raising up to the vertical asymptotes from the points of abscissa Ψ^+ and Π^+. An intersection of F_1 is thus guaranteed with the leftmost branch.

(Z5) In this case the nonnegative part of the function F_2 is a hump joining the points on the S axis with abscissae $S^0_{F_1}$ and Ψ^-. Again two subcases arise, whether $Y = \beta$ does or does not intercept this hump.

(Z5a) Two intersections of $Y = \beta$ with F_2 must occur with abscissae within $[S^0_{F_1}, \Psi^-]$. Then $\widetilde{\Pi}$ is nonnegative in $[S^0_{F_1}, A^-]$ and $[A^+, S^\infty_{F_1})$ and similarly for $\widehat{\Pi}$, but for the fact that at A^- and A^+ vertical asymptotes occur and at $S^\infty_{F_1}$ there is a zero. For Π similar properties hold, but for the latter, and finally Φ results nonnegative in $[S^0_{F_1}, A^-]$ and in $[A^+, \Psi^-]$. The intersection with F_1 exists always in this latter interval, and one further can occur in the former, if the condition (14) is satisfied.

(Z5b) If $Y = \beta$ lies entirely above F_2, $\widetilde{\Pi} > 0$ on the whole $I_{F_1} > 0$, $\widehat{\Pi} \geq 0$ in it, with $\widehat{\Pi}(S^\infty_{F_1}) = 0$, Π shares the same property and moreover $\Pi(S^0_{F_1}) = \Pi(S^\infty_{F_1}) = S^\infty_{F_1} + \beta^{-1}$, and finally Φ has a nonnegative hump exactly in the same interval where F_2 does, $[S^0_{F_1}, \Psi^-]$. To have an intercept with F_1 we must once more require the slope condition (15).

Note that the conditions (14) and (15) can be explicitly evaluated, and namely simplify to

$$F_1'(S^0_{F_1}) = \gamma C \frac{S^0_{F_1} - S^-_{F_1}}{S^\infty_{F_1} - S^0_{F_1}}, \quad \Phi'(S^0_{F_1}) = \frac{1}{b\mu} F_2'(S^0_{F_1}) \left(S^0_{F_1} + \frac{K_1 \delta}{\beta} \right), \quad F_2'(S^0_{F_1}) = -C\Phi(S^0_{F_1}). \tag{16}$$

3.3 Stability analysis

The Jacobian J of system (1) has three vanishing entries, namely $J_{12} = J_{34} = J_{43} = 0$. The other components are

$$J_{11} = a\left(1 - \frac{2S}{K}\right) - \frac{d_1\alpha_1 Z}{(d_1+S)^2} - \frac{\beta V}{K_1+V},\ J_{13} = -\frac{\alpha_1 S}{d_1+S},\ J_{14} = -\frac{K_1\beta S}{(K_1+V)^2},$$
$$J_{21} = \frac{\beta V}{K_1+V} + \frac{\alpha_2\gamma IZ}{(d_2+I+\gamma S)^2},\ J_{22} = -\frac{\alpha_2 Z(d_2+\gamma S)}{(d_2+I+\gamma S)^2} - \mu,\ J_{23} = -\frac{\alpha_2 I}{d_2+I+\gamma S},$$
$$J_{24} = \frac{K_1\beta S}{(K_1+V)^2},\ J_{31} = \frac{\lambda_1 d_1\alpha_1 Z}{(d_1+S)^2} + \frac{\lambda_2\alpha_2\gamma IZ}{(d_2+I+\gamma S)^2},\ J_{32} = -\frac{\lambda_2\alpha_2 Z(d_2+\gamma S)}{(d_2+I+\gamma S)^2},$$
$$J_{33} = \frac{\lambda_1\alpha_1 S}{d_1+S} - \frac{\lambda_2\alpha_2 I}{d_2+I+\gamma S} - \nu,\ J_{41} = -\frac{\beta V}{K_1+V},\ J_{42} = b\mu,\ J_{44} = -\left(\delta + \frac{K_1\beta S}{(K_1+V)^2}\right).$$

The origin E_0 is unstable, having the eigenvalues $a > 0$, $-\mu$, $-\nu$ and $-\delta$. Two eigenvalues factorize in the case of E_1,

$$-a < 0, \quad \frac{\lambda_1\alpha_1 K}{d_1+K} - \nu,$$

and the Routh-Hurwitz conditions on the remaining minor become

$$\frac{\beta K}{K_1} + \delta + \mu > 0, \quad \mu\left(\delta - \frac{(b-1)\beta K}{K_1}\right) > 0.$$

Stability thus holds if the following conditions are satisfied:

$$\delta K_1 - \beta(b-1)K > 0,\ \nu d_1 - K(\lambda_1\alpha_1 - \nu) > 0. \tag{17}$$

At E_2 the characteristic equation factorizes into the product of two quadratic equations,

$$\rho^2 + C_1\rho + C_2 = 0, \quad \rho^2 + C_3\rho + C_4 = 0, \tag{18}$$

with $C_1 = J_{22}(E_2) + J_{44}(E_2) > 0$, $C_2 = J_{22}(E_2)J_{44}(E_2) - J_{14}(E_2)J_{42}(E_2)$, $C_3 = -J_{11}(E_2)$, $C_4 = J_{13}(E_2)J_{31}(E_2) > 0$, because the Jacobian entries simplify as follows:

$$J_{11}(E_2) = \frac{aS_2}{K} - \frac{\alpha_1 S_2 Z_2}{(d_1+S_2)^2}, \quad J_{13}(E_2) = \frac{\alpha_1 S_2}{d_1+S_2}, \quad J_{14}(E_2) = J_{24} = \frac{\beta S_2}{K_1}, \quad J_{42}(E_2) = b\mu,$$
$$J_{22}(E_2) = \frac{\alpha_2 Z_2}{d_2+\gamma S_2} + \mu, \quad J_{31}(E_2) = \frac{\lambda_1 d_1\alpha_1 Z_2}{(d_1+S_2)^2}, \quad J_{32}(E_2) = \frac{\lambda_2\alpha_2 Z_2}{d_2+\gamma S_2}, \quad J_{44}(E_2) = \frac{\beta S_2}{K_1} + \delta.$$

In view of $C_1 > 0$ and $C_4 > 0$, all roots of the equations in (18) are either negative or have negative real parts if and only if C_2 and C_3 are positive. Thus, the equilibrium E_2 is locally asymptotically stable provided

$$\delta\left(\frac{\alpha_2 Z_2}{d_2+\gamma S_2} + \mu\right) + \frac{\beta S_2}{K_1}\frac{\alpha_2 Z_2}{d_2+\gamma S_2} - \frac{\mu(b-1)\beta S_2}{K_1} > 0,\ a(d_1+S_2)^2 > K\alpha_1 Z_2. \tag{19}$$

One eigenvalue of the Jacobian $J(E_3)$ factorizes to provide the necessary stability condition

$$\frac{\lambda_1\alpha_1 S_3}{d_1+S_3} < \frac{\lambda_2\alpha_2 I_3}{d_2+I_3+\gamma S_3} + \nu \tag{20}$$

and other three are given by roots of the cubic

$$\rho^3 + B_1\rho^2 + B_2\rho + B_3 = 0, \tag{21}$$

where

$$B_1 = J_{11}(E_3) + J_{22}(E_3) + J_{44}(E_3),$$

$$B_2 = J_{11}(E_3)J_{22}(E_3) + J_{11}(E_3)J_{44}(E_3) + J_{22}(E_3)J_{44}(E_3) - J_{14}(E_3)J_{42}(E_3) - J_{14}(E_3)J_{21}(E_3),$$

$$B_3 = J_{11}(E_3)J_{22}(E_3)J_{44}(E_3) - J_{11}(E_3)J_{14}(E_3)J_{42}(E_3) + J_{14}(E_3)J_{21}(E_3)J_{42}(E_3) - J_{14}(E_3)J_{21}(E_3)J_{22}(E_3)$$

with

$$J_{11}(E_3) = \frac{aS_3}{K}, \quad J_{13}(E_3) = \frac{\alpha_1 S_3}{d_1+S_3}, \quad J_{14}(E_3) = J_{24}(E_3) = \frac{K_1\beta S_3}{(K_1+V_3)^2},$$
$$J_{21}(E_3) = J_{41}(E_3) = \frac{\beta V_3}{K_1+V_3}, \quad J_{22} = \mu, \quad J_{23}(E_3) = \frac{\alpha_2 I_3}{d_2+I_3+\gamma S_3},$$
$$J_{33}(E_3) = \frac{\lambda_1\alpha_1 S_3}{d_1+S_3} - \frac{\lambda_2\alpha_2 I_3}{d_2+I_3+\gamma S_3} - \nu, \quad J_{42}(E_3) = b\mu, \quad J_{44}(E_3) = \frac{K_1\beta S_3}{(K_1+V_3)^2} + \delta.$$

The roots of equation (21) are either negative or with negative real parts if and only if the Routh-Hurwitz conditions criterion are satisfied,

$$B_1 > 0,\ B_3 > 0,\ B_1B_2 - B_3 > 0, \tag{22}$$

so that in such case and if (20) holds, E_3 is locally asymptotically stable.

At coexistence, note that the Jacobian has only one simplification, namely $J_{33}(E^*) = J^*_{33} = 0$. The associated characteristic equation is

$$\rho^4 + \sigma_1\rho^3 + \sigma_2\rho^2 + \sigma_3\rho + \sigma_4 = 0, \tag{23}$$

where

$$\sigma_1 = J^*_{11} + J^*_{22} + J^*_{44},$$

$$\sigma_2 = J^*_{11}J^*_{22} + J^*_{11}J^*_{44} + J^*_{13}J^*_{31} - J^*_{14}J^*_{41} + J^*_{22}J^*_{44} - J^*_{23}J^*_{32} - J^*_{24}J^*_{42},$$

$$\sigma_3 = J^*_{11}J^*_{22}J^*_{44} - J^*_{11}J^*_{23}J^*_{32} - J^*_{11}J^*_{24}J^*_{42} + J^*_{13}J^*_{31}J^*_{22} + J^*_{13}J^*_{31}J^*_{44}$$
$$-J^*_{13}J^*_{21}J^*_{32} + J^*_{14}J^*_{21}J^*_{42} - J^*_{14}J^*_{22}J^*_{41} - J^*_{23}J^*_{32}J^*_{44},$$

$$\sigma_4 = J^*_{13}J^*_{22}J^*_{31}J^*_{44} - J^*_{11}J^*_{23}J^*_{32}J^*_{44} - J^*_{13}J^*_{21}J^*_{32}J^*_{44} - J^*_{13}J^*_{24}J^*_{31}J^*_{42}$$
$$+J^*_{13}J^*_{24}J^*_{32}J^*_{41} - J^*_{14}J^*_{23}J^*_{31}J^*_{42} + J^*_{14}J^*_{23}J^*_{32}J^*_{41}.$$

Again using the Routh-Hurwitz criterion, E^*, whenever feasible, is locally asymptotically stable if and only if the following conditions are satisfied,

$$\sigma_1 > 0,\ \sigma_4 > 0,\ \sigma_1\sigma_2 - \sigma_3 > 0,\ \sigma_3(\sigma_1\sigma_2 - \sigma_3) - \sigma_1^2\sigma_4 > 0. \tag{24}$$

In summary, we have the following theorem.

Theorem 2 *The origin E_0 is always unstable. The phytoplankton only equilibrium E_1 is stable provided condition (17) holds. The disease-free equilibrium E_2, if feasible, is stable if the conditions in (19) hold. The zooplankton-free equilibrium E_3, if feasible, is stable if conditions (20) and (22) hold. The coexistence equilibrium E^*, if feasible, is stable if the conditions in (24) hold.*

3.4 Nonexistence of periodic solutions

Periodic solutions can be ruled out using the approach of [59]. We have the following result.

Theorem 3 *The system (1) has no periodic solution around the interior equilibrium E^* if*

$$\begin{aligned} a + \alpha_1 + \frac{K_1\beta S^*}{(K_1+V^*)^2} + b\mu + \frac{\alpha_1 S^*}{d_1+S^*} + \frac{\beta V^*}{K_1+V^*} + \frac{\alpha_2 I^*}{d_2+I^*+\gamma S^*} + \frac{\lambda_2\alpha_2\{d_2+\gamma(S^*+I^*)\}Z^*}{(d_2+I^*+\gamma S^*)^2} \\ + \frac{\lambda_1\alpha_1 d_1 Z^*}{(d_1+S^*)^2} < \min\left\{\beta+\mu+\frac{\alpha_1 Z^*}{d_1}+\frac{2aS^*}{K}+\frac{\alpha_2 Z^*}{d_2+\gamma S^*},\ \mu+\frac{\alpha_2 Z^*}{d_2+\gamma S^*}, \beta+\frac{\alpha_1 Z^*}{d_1}+\frac{2aS^*}{K}, \right. \\ \left. \beta\left(1+\frac{S^*}{K_1}\right)+\delta+\frac{2aS^*}{K}+\frac{\alpha_1 Z^*}{d_1},\ \mu+\delta+\frac{\beta S^*}{K_1}+\frac{\alpha_2 Z^*}{d_2+\gamma S^*},\ \delta+\frac{\beta S^*}{K_1}\right\}. \end{aligned} \tag{25}$$

Proof The second additive compound matrix of the Jacobian of the system (1) is given by

$$J^{[2]} = \begin{pmatrix} F_S+G_I & G_Z & G_V & -F_Z & -F_V & 0 \\ H_I & F_S & 0 & 0 & 0 & -F_V \\ L_I & 0 & F_S+L_V & 0 & 0 & F_Z \\ -H_S & G_S & 0 & G_I & 0 & -G_V \\ -L_S & 0 & G_S & 0 & G_I+L_V & G_Z \\ 0 & -L_S & H_S & -L_I & H_I & L_V \end{pmatrix},$$

where

$$F_S = -J^*_{11},\ F_Z = -J^*_{13},\ F_V = -J^*_{14},\ G_S = J^*_{21},\ G_I = -J^*_{22},\ G_Z = -J^*_{23},$$
$$G_V = J^*_{24},\ H_S = J^*_{31},\ H_I = -J^*_{32},\ L_S = -J^*_{41},\ L_I = J^*_{42},\ L_V = -J^*_{44}.$$

Let $|X|_\infty = \sup_i |X_i|$. The logarithmic norm $\mu_\infty(J^{[2]})$ of $J^{[2]}$ endowed with the vector norm $|X|_\infty$ is the supremum of $F_S + G_I + |G_Z| + |G_V| + |F_Z| + |F_V|$, $|H_I| + F_S + |F_V|$, $|L_I| + F_S + L_V + |F_Z|$, $|H_S| + |G_S| + G_I + |G_V|$, $|L_S| + |G_S| + G_I + L_V + |G_Z|$ and $|L_S| + |H_S| + |L_I| + |H_I| + |L_V|$.

Now, $(F_S + G_I + |G_Z| + |G_V| + |F_Z| + |F_V|)_{E^*} < 0$ if

$$a + \alpha_1 + \frac{K_1\beta S^*}{(K_1+V^*)^2} + \frac{\alpha_2 I^*}{d_2 + I^* + \gamma S^*} < \beta + \frac{2aS^*}{K} + \mu + \frac{\alpha_1 Z^*}{d_1} + \frac{\alpha_2 Z^*}{d_2 + \gamma S^*};$$

similarly $(|H_S| + F_S + |F_V|)_{E^*} < 0$ if

$$a + \frac{K_1\beta S^*}{(K_1+V^*)^2} + \frac{\lambda_2\alpha_2(d_2+\gamma S^*)Z^*}{(d_2 + I^* + \gamma S^*)^2} < \frac{2aS^*}{K} + \beta + \frac{\alpha_1 Z^*}{d_1};$$

also, $(|L_I| + F_S + L_V + |F_Z|)_{E^*} < 0$ if

$$a + b\mu + \frac{\alpha_1 S^*}{d_1 + S^*} < \beta + \delta + \frac{2aS^*}{K} + \frac{\alpha_1 Z^*}{d_1} + \frac{\beta S^*}{K_1};$$

further $(|H_S| + |G_S| + G_I + |G_V|)_{E^*} < 0$ if

$$\frac{\lambda_1\alpha_1 d_1 Z^*}{(d_1+S^*)^2} + \frac{\alpha_2\gamma I^* Z^*}{(d_2 + I^* + \gamma S^*)^2} + \frac{\beta V^*}{K_1 + V^*} + \frac{K_1\beta S^*}{(K_1+V^*)^2} < \mu + \frac{\alpha_2 Z^*}{d_2 + \gamma S^*};$$

then $(|L_S| + |G_S| + G_I + L_V + |G_Z|)_{E^*} < 0$ if

$$\frac{\beta V^*}{K_1 + V^*} + \frac{\alpha_2\gamma I^* Z^*}{(d_2 + I^* + \gamma S^*)^2} + \frac{\alpha_2 I^*}{d_2 + I^* + \gamma S^*} < \mu + \delta + \frac{\beta S^*}{K_1} + \frac{\alpha_2 Z^*}{d_2 + \gamma S^*};$$

and finally $(|L_S| + |H_S| + |L_I| + |H_I| + L_V)_{E^*} < 0$ if

$$b\mu + \frac{\beta V^*}{K_1 + V^*} + \frac{\lambda_1\alpha_1 d_1 Z^*}{(d_1+S^*)^2} + \frac{\lambda_2\alpha_2\{d_2 + \gamma(S^*+I^*)\}Z^*}{(d_2 + I^* + \gamma S^*)^2} < \delta + \frac{\beta S^*}{K_1}.$$

Hence the condition (25).

3.5 Hopf-bifurcation analysis

In this section, we show that at the coexistence equilibrium E^* a Hopf-bifurcation arises, by taking the intensity of avoidance, γ, as bifurcation parameter while keeping the other parameters fixed. More specifically, we have the following result.

Theorem 4 *The coexistence equilibrium E^* enters into Hopf-bifurcation as $\gamma \geq 0$ crosses the critical threshold γ^*, this value being defined as a positive root of the equation $\psi(\gamma) = 0$, where $\psi : (0, \infty) \to \mathbb{R}$ represents the following continuously differentiable function of γ:*

$$\psi(\gamma) = \sigma_1(\gamma)\sigma_2(\gamma)\sigma_3(\gamma) - \sigma_3^2(\gamma) - \sigma_4(\gamma)\sigma_1^2(\gamma).$$

The Hopf-bifurcation occurs if and only if the condition

$$\sigma_1^2(\sigma_1\sigma_4' - \sigma_2'\sigma_3) - (\sigma_1\sigma_2 - 2\sigma_3)(\sigma_1\sigma_3' - \sigma_1'\sigma_3) \neq 0, \tag{26}$$

holds and all other eigenvalues have negative real parts.

Proof Using the condition $\psi(\gamma^*) = 0$, the characteristic equation (23) can be rewritten as

$$\left(\rho^2 + \frac{\sigma_3}{\sigma_1}\right)\left(\rho^2 + \sigma_1\rho + \frac{\sigma_1\sigma_4}{\sigma_3}\right) = 0. \tag{27}$$

Let the roots of the above equation be denoted by ρ_i, $i = 1, 2, 3, 4$ and the pair of purely imaginary roots at $\gamma = \gamma^*$ be ρ_1 and ρ_2. We then have

$$\rho_3 + \rho_4 = -\sigma_1, \tag{28}$$

$$\omega_0^2 + \rho_3\rho_4 = \sigma_2, \tag{29}$$

$$\omega_0^2(\rho_3 + \rho_4) = -\sigma_3, \tag{30}$$

$$\omega_0^2\rho_3\rho_4 = \sigma_4, \tag{31}$$

where $\omega_0 = Im\big(\rho_1(\gamma^*)\big)$. By (31) we find $\omega_0 = \sqrt{\sigma_3\sigma_1^{-1}}$. Now, if ρ_3 and ρ_4 are complex conjugate then from (28), it follows that $2Re\big(\rho_3\big) = -\sigma_1$; if they are real roots, recalling that $\sigma_4 > 0$ by the Routh-Hurwitz conditions, then by (31) they must have the same sign and from (28) they must be negative, i.e. $\rho_3 < 0$ and $\rho_4 < 0$. To complete the discussion, it remains to verify the transversality condition.

As $\psi(\gamma^*)$ is a continuous function of all its roots, there exists an open interval $I_{\gamma^*} = (\gamma^* - \epsilon, \gamma^* + \epsilon)$, where ρ_1 and ρ_2 are complex conjugate for all $\gamma \in I_{\gamma^*}$. Let their general forms in this neighborhood be

$$\rho_1(\gamma) = \chi(\gamma) + i\xi(\gamma),\ \rho_2(\gamma) = \chi(\gamma) - i\xi(\gamma).$$

Substituting $\rho_j(\gamma) = \chi(\gamma) \pm i\xi(\gamma)$, into the characteristics equation $D(\rho) = 0$ and calculating the derivative, we have

$$L_1(\gamma)\chi'(\gamma) - L_2(\gamma)\xi'(\gamma) + L_3(\gamma) = 0,\ L_2(\gamma)\chi'(\gamma) + L_1(\gamma)\xi'(\gamma) + L_4(\gamma) = 0,$$

where

$$L_1(\gamma) = 4\chi^3 - 12\chi\xi^2 + 3\sigma_1(\chi^2 - \xi^2) + 2\sigma_2\chi + \sigma_3,\ L_2(\gamma) = 12\chi^2\xi - 4\xi^3 + 6\sigma_1\chi\xi + 2\sigma_2\xi,$$
$$L_3(\gamma) = \sigma_1'\chi^3 - 3\sigma_1'\chi\xi^2 + \sigma_2'(\chi^2 - \xi^2) + \sigma_3'\chi + \sigma_4',\ L_4(\gamma) = 3\sigma_1'\chi^2\xi - \sigma_1'\xi^3 + 2\sigma_2'\chi\xi + \sigma_3'\xi.$$

For $\gamma = \gamma^*$, we obtain

$$L_1(\gamma^*) = -2\sigma_3,\ L_2(\gamma^*) = 2\sqrt{\frac{\sigma_3}{\sigma_1}}\left\{\sigma_2 - \frac{2\sigma_3}{\sigma_1}\right\},$$
$$L_3(\gamma^*) = \sigma_4' - \frac{\sigma_2'\sigma_3}{\sigma_1},\ L_4(\gamma^*) = \sqrt{\frac{\sigma_3}{\sigma_1}}\left(\sigma_3' - \frac{\sigma_1'\sigma_3}{\sigma_1}\right).$$

Solving for $\chi'(\gamma)$ at $\gamma = \gamma^*$, we have

$$\frac{d}{d\gamma}(Re\rho_j(\gamma))|_{\gamma=\gamma^*} = \chi'(\gamma^*) = -\frac{L_2(\gamma^*)L_4(\gamma^*) + L_1(\gamma^*)L_3(\gamma^*)}{L_1^2(\gamma^*) + L_2^2(\gamma^*)}$$
$$= \frac{\sigma_1^2(\sigma_1\sigma_4' - \sigma_2'\sigma_3) - (\sigma_1\sigma_2 - 2\sigma_3)(\sigma_1\sigma_3' - \sigma_1'\sigma_3)}{2\sigma_1^3\sigma_3 + 2(\sigma_1\sigma_2 - 2\sigma_3)^2} \neq 0$$

if (26) is satisfied. Thus the transversality condition holds and hence the claim.

To better understand the nature of the instability, we determine the initial period and the amplitude of the oscillatory solutions. From (28)−(31), solving (30) for ω^2 and substituting from (28) we get $\omega^2 = \sigma_3\sigma_1^{-1}$. Obtaining σ_4 from (31) and combining with the previous result, we find $\sigma_4 = \sigma_3\rho_3\rho_4\sigma_1^{-1}$. The quantity $\rho_3\rho_4$ is obtained then from (29), and thus leads to the expression $\sigma_4 = \sigma_3(\sigma_1\sigma_2 - \sigma_3)\sigma_1^{-2}$. Then relaxing it to $\sigma_4(\psi) = \psi\sigma_4$ and substituting into equation (23), if ρ depends continuously on ψ, we can rewrite equation (23) as

$$\rho^4 + \sigma_1\rho^3 + \sigma_2\rho^2 + \sigma_3\rho + \frac{\psi\sigma_3(\sigma_1\sigma_2 - \sigma_3)}{\sigma_1^2} = 0. \tag{32}$$

At $\psi = \psi^* = 1$, because $\sigma_1^2\sigma_4 = \sigma_3(\sigma_1\sigma_2 - \sigma_3)$, equation (23) factorizes into the form (27) which has a pair of purely imaginary roots, $\rho(\psi^*) = \pm i\sqrt{\sigma_3\sigma_1^{-1}}$ while the other two roots are either negative or have negative real parts. This substantiates the claim that the Hopf-bifurcation is present.

Further, if $\psi \in (0, 1)$, then $\sigma_1^2\sigma_4 - \sigma_3(\sigma_1\sigma_2 - \sigma_3)$ is positive, which assures stability, and conversely for $\psi > 1$, we obtain instability.

Observe now that ρ is a function of ψ. We differentiate equation (32) with respect to ψ, denoting this operation by a prime. By setting $\psi = \psi^* + \epsilon^2\xi$, where $|\epsilon| \ll 1$ and $\xi = \pm 1$, then $\rho(\psi) = \rho(\psi^* + \epsilon^2\xi)$ so that expanding in Taylor series of ρ around ψ^* up to the first order, we find

$$\rho(\psi) = \rho(\psi^*) + \rho'(\psi^*)\epsilon^2\xi + O(\epsilon^4). \tag{33}$$

Replacing $\rho(\psi^*)$ by $i \pm \sqrt{\frac{\sigma_3}{\sigma_1}}$ in the derivative and conjugating the expression for the derivative we get equation

$$\rho'(\psi^*) \equiv \frac{\sigma_1\sigma_3(\sigma_1\sigma_2 - \sigma_3)}{2[\sigma_1^3\sigma_3 + (\sigma_1\sigma_2 - 2\sigma_3)^2]} \pm i\sqrt{\frac{\sigma_3}{\sigma_1}}\frac{(\sigma_1\sigma_2 - \sigma_3)(\sigma_1\sigma_2 - 2\sigma_3)}{2[\sigma_1^3\sigma_3 + (\sigma_1\sigma_2 - 2\sigma_3)^2]}. \tag{34}$$

Using the fact that

$$\Re(\rho(\psi^*)) = 0, \quad \Re(\rho'(\psi^*)) = \frac{\sigma_1\sigma_3(\sigma_1\sigma_2 - \sigma_3)}{2[\sigma_1^3\sigma_3 + (\sigma_1\sigma_2 - 2\sigma_3)^2]} > 0$$

and substituting $\rho(\psi^*)$ and $\rho'(\psi)$ into equation (33), we obtain the approximation

$$\begin{aligned}\rho(\psi^*) &= \rho(\psi^*) + \rho'(\psi^*)\epsilon^2\xi \\ &= \frac{\sigma_1\sigma_3(\sigma_1\sigma_2 - \sigma_3)\epsilon^2\xi}{2[\sigma_1^3\sigma_3 + (\sigma_1\sigma_2 - 2\sigma_3)^2]} \pm i\sqrt{\frac{\sigma_3}{\sigma_1}}\left(1 + \frac{(\sigma_1\sigma_2 - \sigma_3)(\sigma_1\sigma_2 - 2\sigma_3)\epsilon^2\xi}{2[\sigma_1^3\sigma_3 + (\sigma_1\sigma_2 - 2\sigma_3)^2]}\right) + O(\epsilon^4). \qquad (35)\end{aligned}$$

Setting $\epsilon = \sqrt{|\psi - \psi^*| \times |\xi|^{-1}}$, the initial period and amplitude of the oscillations associated with the loss of stability when $\psi > \psi^*$ respectively are

$$\frac{2\pi}{\sqrt{\frac{\sigma_3}{\sigma_1}}\left(1 + \frac{(\sigma_1\sigma_2 - \sigma_3)(\sigma_1\sigma_2 - 2\sigma_3)\epsilon^2\xi}{2[\sigma_1^3\sigma_3 + (\sigma_1\sigma_2 - 2\sigma_3)^2]}\right)}, \quad \exp\left(\frac{\sigma_1\sigma_3(\sigma_1\sigma_2 - \sigma_3)\epsilon^2\xi}{2[\sigma_1^3\sigma_3 + (\sigma_1\sigma_2 - 2\sigma_3)^2]}\right).$$

4 Simulations of the ecoystem behavior

Here, we report the simulations to investigate the behavior of system (1), performed using the Matlab variable step Runge-Kutta solver ode45. The set of parameter values are chosen within the range prescribed in various previous literature sources [14,15,52], and are given in Table 1.

4.1 Sensitivity analysis

To assess the sensitivity of the solutions to variations in the model parameters partial rank correlation coefficient (PRCC), a global sensitivity analysis technique that is proven to be the most reliable and efficient among the sampling-based methods, is utilized. The PRCC determines the effect of changes in a specific parameter, by discounting linearly the influences over the other parameters, on the reference model output [60]. In order to obtain the PRCC values, Latin Hypercube Sampling (LHS) is chosen for the input parameters by performing a stratified sampling without replacement. In the current study, a uniform distribution is assigned to each model parameter and sampling is performed independently. The range for each parameter is initially set to $\pm 25\%$ of the nominal values given in Table 1. A total of 200 simulations are considered, wherein a set of parameter values are selected from the uniform distribution.

Note that the PRCC values lie between -1 and 1. Positive (negative) values indicate a positive (negative) correlation of the parameter with the model output. A positive (negative) correlation implies that a positive (negative) change in the parameter will increase (decrease) the model output. The larger

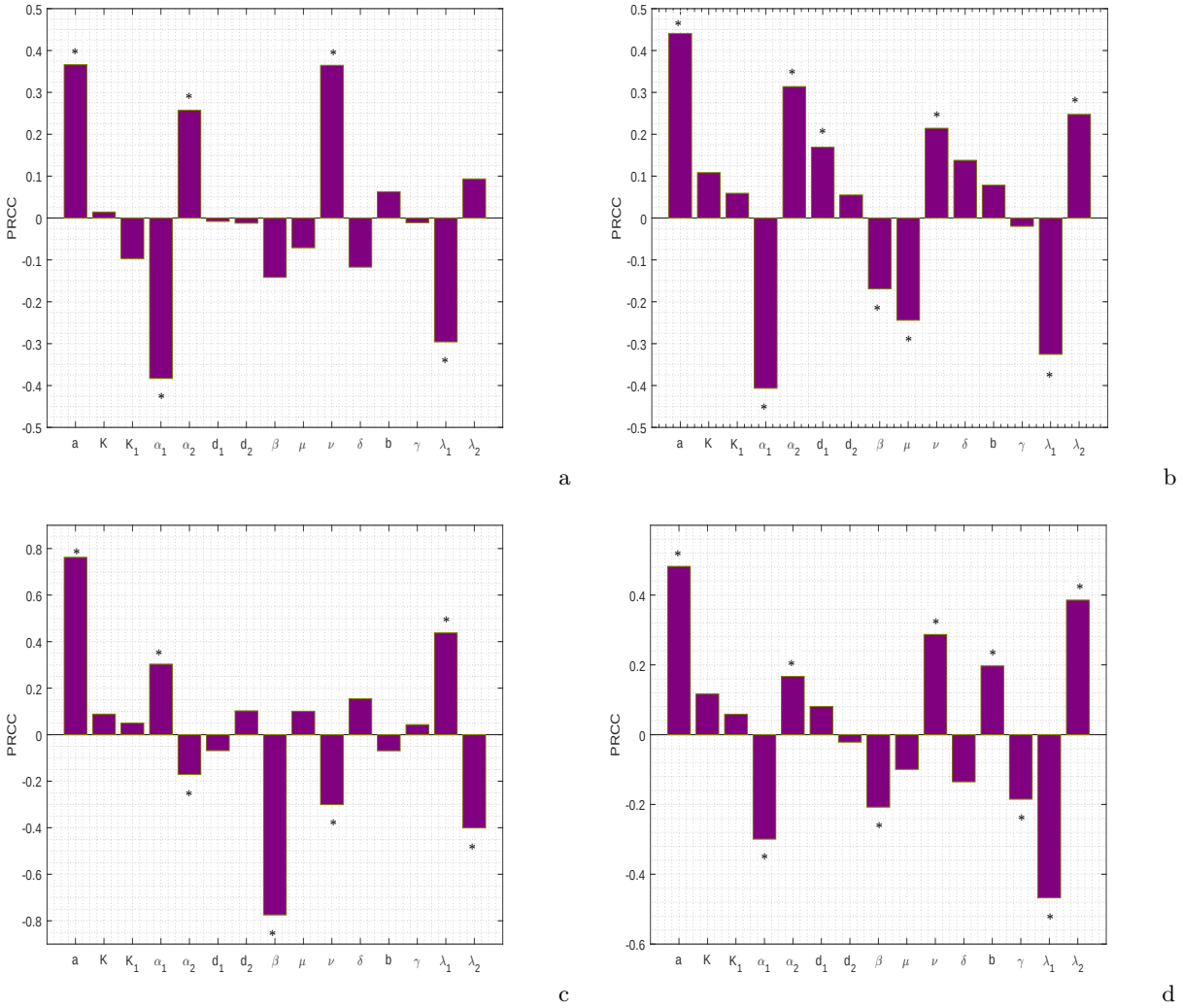

Fig. 2 Effect of uncertainty of the model (1) on (a) S, (b) I, (c) Z and (d) V. Significant parameters are marked by * for $p < 0.01$. Baseline values of the parameter are the same as in Table 1.

the absolute value of the PRCC, the greater the correlation of the parameter with the output. The bar diagram of the PRCC values of susceptible phytoplankton, infected phytoplankton, zooplankton and free viruses against the parameters is depicted in Fig. 2. It therefore emerges that susceptible phytoplankton is significantly correlated with the model parameters a, α_1, α_2, ν and λ_1, while for the infected phytoplankton, the most influential parameters appear to be a, α_1, α_2, d_1, β, μ, ν, λ_1 and λ_2. Further, the parameters a, α_1, α_2, β, ν, λ_1 and λ_2 instead significantly affect zooplankton. Finally, free viruses are mostly dependent on the parameters a, α_1, α_2, β, ν, b, γ, λ_1 and λ_2.

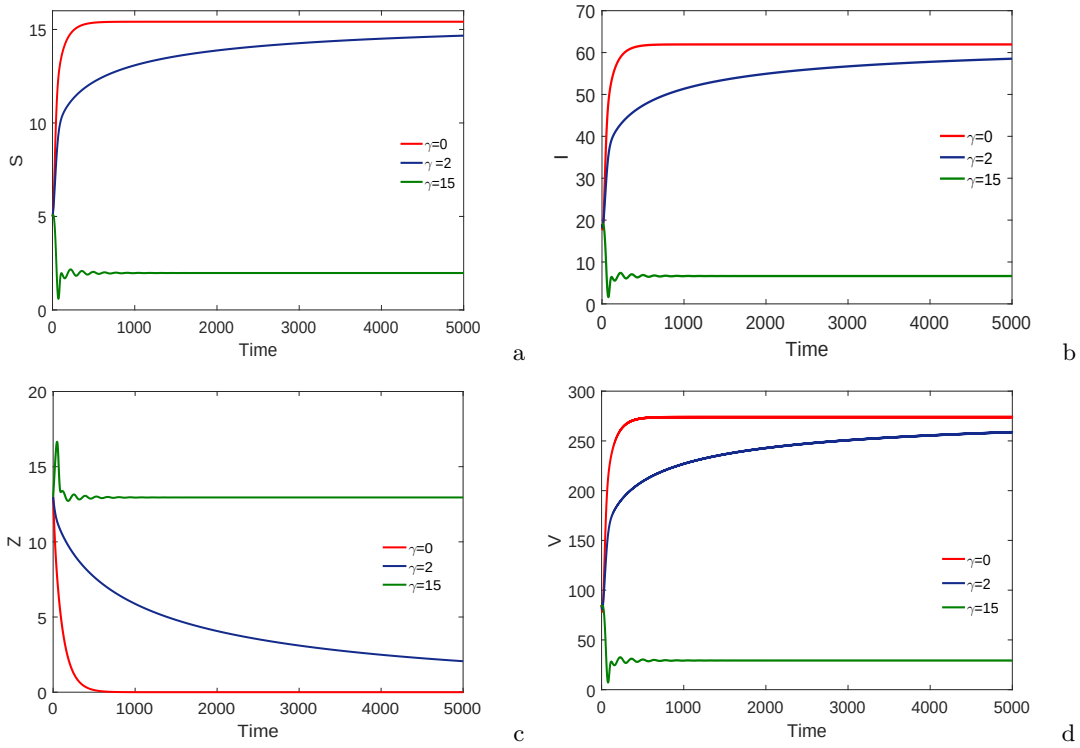

Fig. 3 Variations of susceptible phytoplankton (S), infected phytoplankton (I), zooplankton (Z) and free-viruses (V) with respect to time for different values of γ. Rest of the parameter values are the same as in Table 1.

4.2 Effect on the ecosystem behavior on variations of the model parameters

We see the impact of avoidance parameter, γ, on the equilibrium values of each variables of the system (1), Fig. 3. We see that the abundances of susceptible phytoplankton, infected phytoplankton and free-viruses are at higher values when the zooplankton do not discriminate between susceptible and infected phytoplankton. For the non-zero values of γ, the zooplankton discriminate between susceptible and infected phytoplankton. As the value of γ increases, both type of phytoplankton and free-viruses decrease in the system. For very large values of γ, the phytoplankton and free-viruses settle to very low equilibrium values. Interestingly, the zooplankton population become zero for large time in the case when they do not discriminate between susceptible and infected phytoplankton, as the ingestion of infected phytoplankton increases the death rate of zooplankton. As the values of avoidance parameter increases, the zooplankton move away from the infected phytoplankton, and ingest them at a very low rate. This results in lesser death of zooplankton, and hence their abundance increase with increase in the values of γ. For very large values of γ, the zooplankton population attains high equilibrium values.

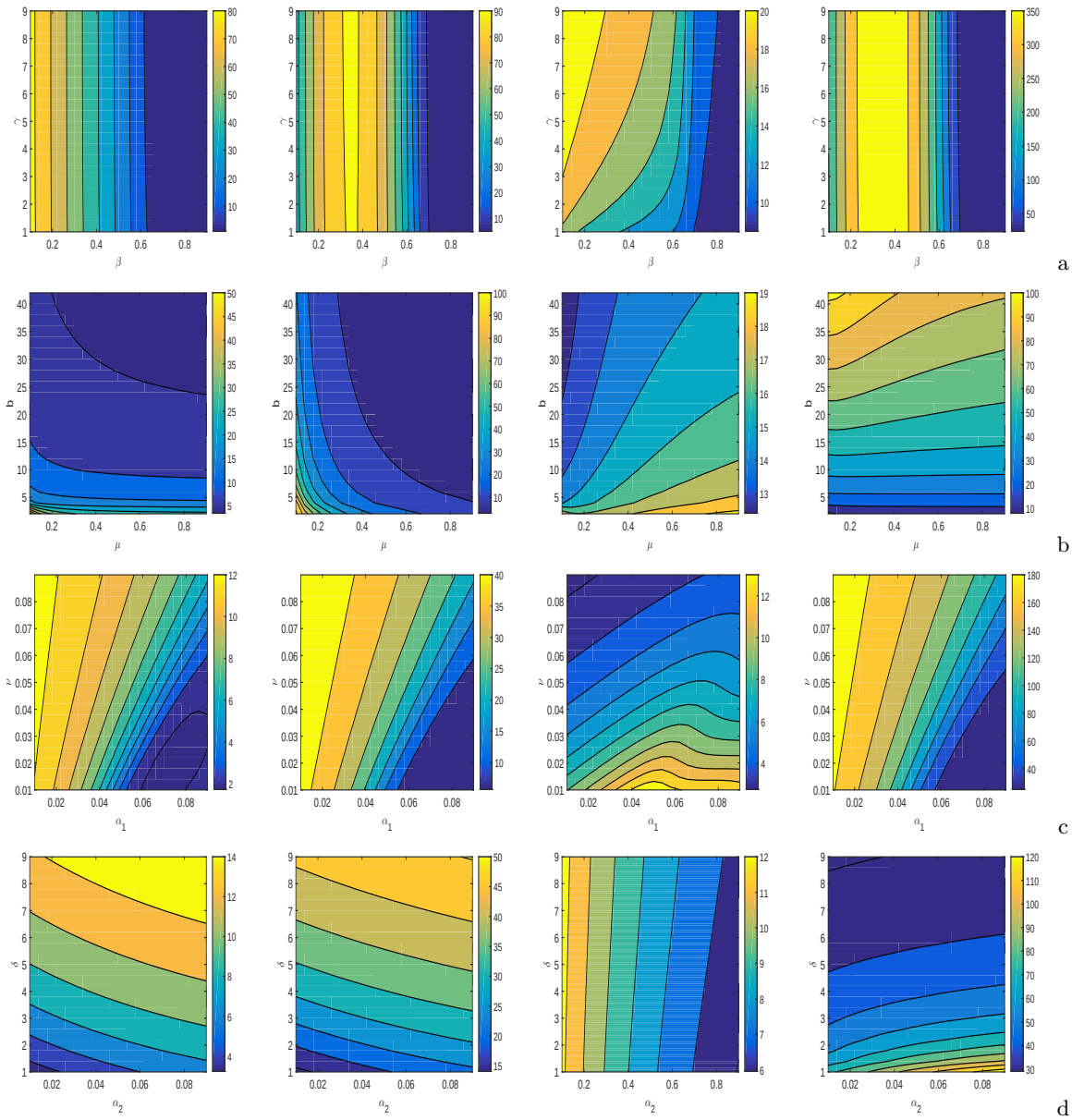

Fig. 4 Contour lines representing the equilibrium values of susceptible phytoplankton (first column), infected phytoplankton (second column), zooplankton (third column) and free viruses (fourth column) as functions of (a) β and γ, (b) μ and b, (c) α_1 and ν, and (d) α_2 and δ. Rest of the parameter values are the same as in Table 1.

Next, we see how equilibrium abundances of ecosystem populations change by varying some of the input parameters, namely β, γ, μ, b, α_1, α_2, ν and δ. By varying two parameters at a time in biologically meaningful regions, we plot contour lines for the surfaces representing the system populations, Fig. 4. It is apparent from Fig. 4(a) that the concentration of zooplankton increases with increase in the intensity of avoidance γ, but for the remaining populations this parameter is instead much less

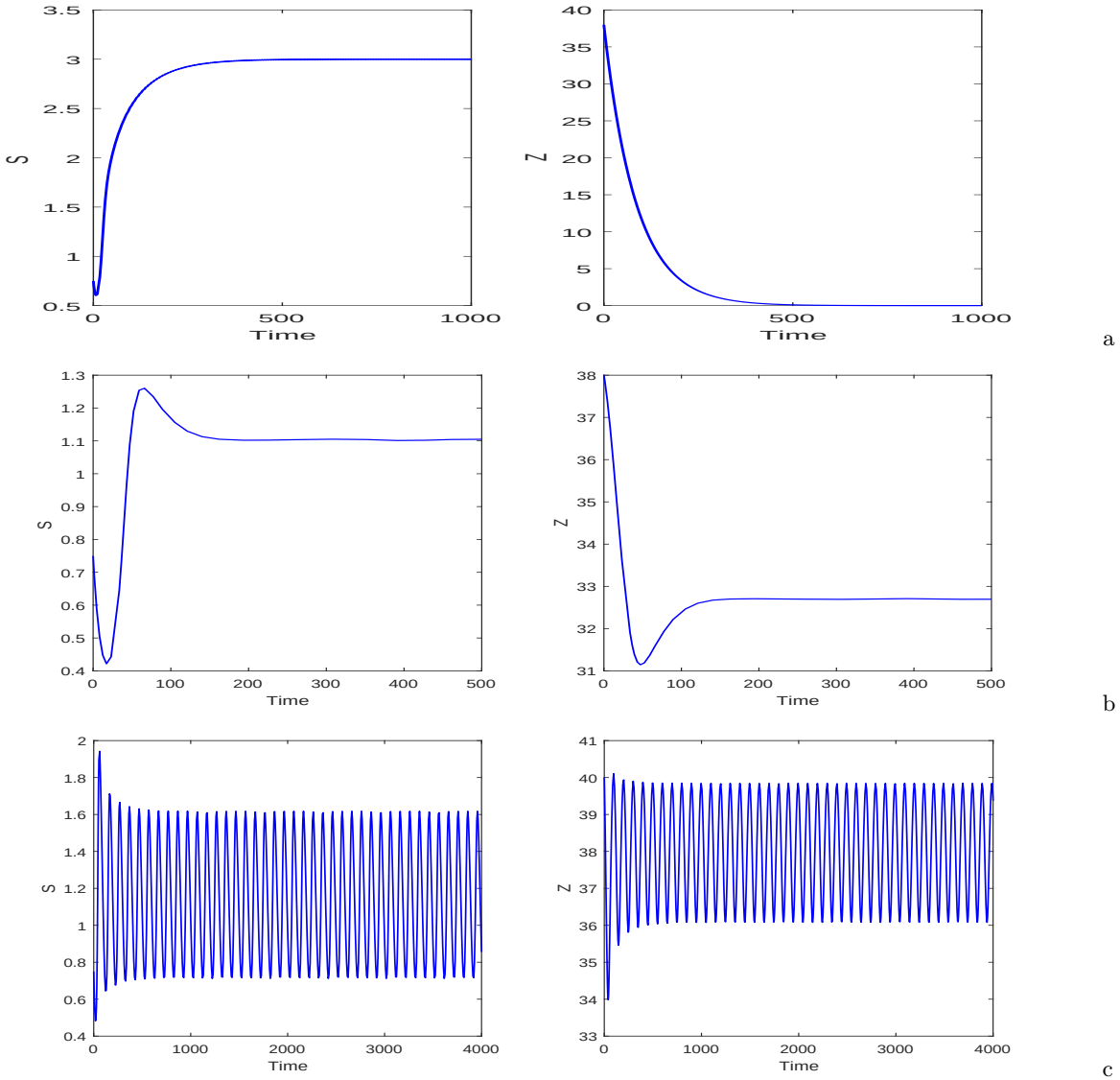

Fig. 5 For virus-free environment ($I = 0$ and $V = 0$) i.e., subsystem (3): (a) zooplankton-free equilibrium is achieved at $K = 3$ and $\lambda_1 = 0.01$. System (3) shows (b) stable coexistence at $K = 3$ and $\lambda_1 = 0.75$, and (c) limit cycle oscillations around the coexistence equilibrium at $K = 4.3$ and $\lambda_1 = 0.75$. Rest of the parameters are at the same values as in Table 1.

influential. On increasing the force of infection β, the concentrations of susceptible phytoplankton and zooplankton decrease while those of infected phytoplankton and free viruses initially increase and then decrease. Fig. 4(b) shows that with an increase in the death rate of infected phytoplankton μ, the concentration of infected phytoplankton decreases but that of zooplankton increases. On increasing the virus-replication factor b, the susceptible phytoplankton and zooplankton populations decrease but the free viruses increase significantly. Looking at Fig. 4(c), we may note that the concentration of

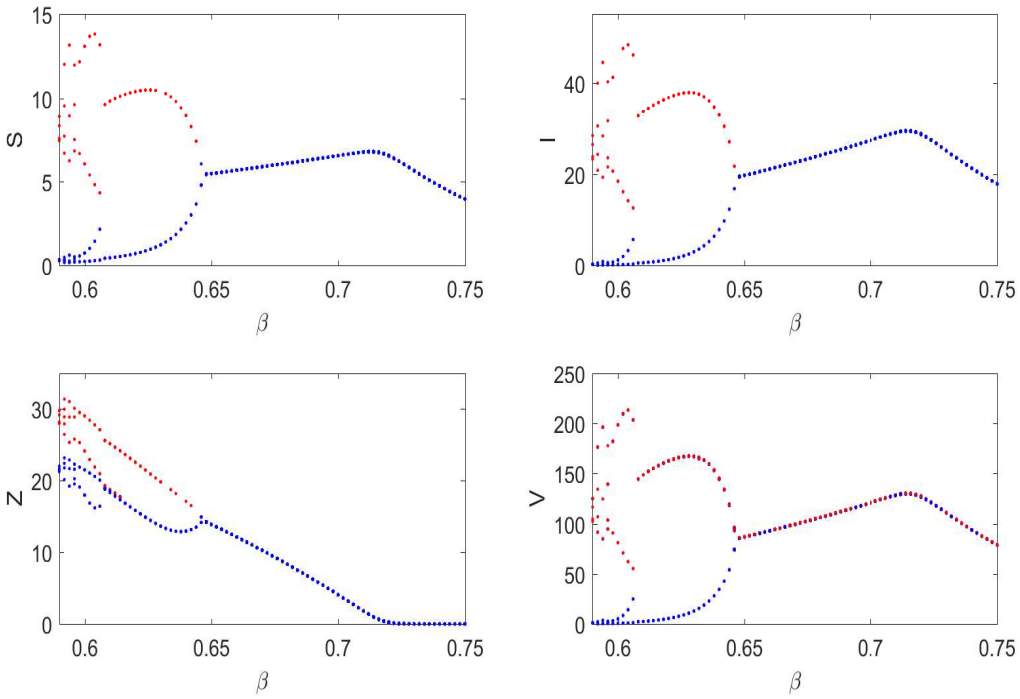

Fig. 6 Bifurcation diagram of the system (1) with respect to force of infection β. Here, the maximum and minimum values of the oscillations are plotted in red and blue colors, respectively. Rest of the parameter values are the same as in Table 1.

susceptible phytoplankton for low values of α_1 decreases by increasing this parameter. The same situations occurs for the infected phytoplankton and the free viruses. However, zooplankton benefits by an increase in the values of α_1. On increasing the zooplankton mortality rate, susceptible phytoplankton, infected phytoplankton and free viruses all increase, but the zooplankton population attains very low equilibrium values. From Fig. 4(d) increasing the values of α_2, leads to higher values of susceptible phytoplankton, infected phytoplankton and viruses, while zooplankton decrease. On increasing the free viruses mortality rate δ, susceptible and infected phytoplankton increase, the latter slightly, while free viruses decrease. Zooplankton essentially are not affected by δ. Looking at the combined effect of α_2 and δ, we observe that along the main diagonal the susceptible phytoplankton increase while free viruses decrease.

4.3 Existence of Hopf-bifurcation and Transcritical bifurcation

First, we investigate the dynamics of the system (1) in the absence of free viruses and infected phytoplankton. For system (3), note that the zooplankton-free equilibrium e_1 is related to the coexistence

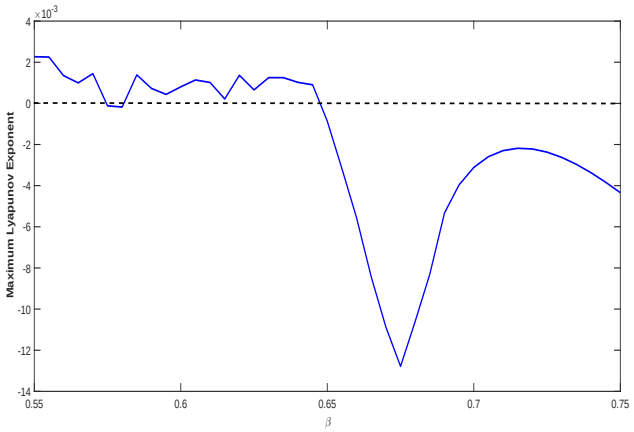

Fig. 7 Variation of the maximum Lyapunov exponent with respect to β for the model (1), where other parameter values are the same as in Table 1. The maximum Lyapunov exponent becomes negative from positive values, which confirms that the system (1) becomes stable from chaotic dynamics for increase in the values of parameter β.

equilibrium e_* via a transcritical bifurcation taking λ_1 as a bifurcation parameter. For low values of λ_1 ($\lambda_1 = 0.01$, $K = 3$), the zooplankton-free equilibrium e_1 is stable, Fig. 5(a), while the zooplankton-free equilibrium e_1 loses its stability and the coexistence equilibrium e_* emanates from the former on increasing the values of λ_1 past a critical threshold, specifically for $\lambda_1 = 0.75$, $K = 3$, Fig. 5(b). Further, observe that on increasing the values of K, specifically $\lambda_1 = 0.75$, $K = 4.3$, the coexistence equilibrium e_* loses its stability and persistent oscillations occur, Fig. 5(c), that are found also by a further increase in the values of K. For the model (1), stability of the disease-free equilibrium E_2 can be obtained with $K = 3.4$, $\beta = 0.12$ and $K_1 = 1.6$, while the remaining parameter values appear in Table 1. Now, we see how dynamics of the system (1) changes on varying the force of infection β, virus replication factor b, intensity of avoidance γ and carrying capacity K, while keeping the values of remaining parameters as in Table 1. We vary the parameter β in the interval [0.59,0.75] and note the different behaviors of system (1), Fig. 6. At $\beta = 0.59$, we observe that the system (1) shows chaotic dynamics; at $\beta = 0.6$ the system exhibits period halving oscillations; at $\beta = 0.62$, the system shows limit cycle oscillation; at $\beta = 0.65$, the system shows stable focus. We find that for large values of β, namely $\beta = 0.74$, the system settles down to the zooplankton-free steady state. Thus, there exists a transcritical bifurcation between equilibria E_3 and E^* where β represents the bifurcation parameter; the former arises while the latter loses its stability as β crosses its critical value from below. The most important mathematical attribute of chaos is the absence of any stable equilibrium point or any stable limit cycle in system dynamics, for which the patterns never repeat themselves. We also report the

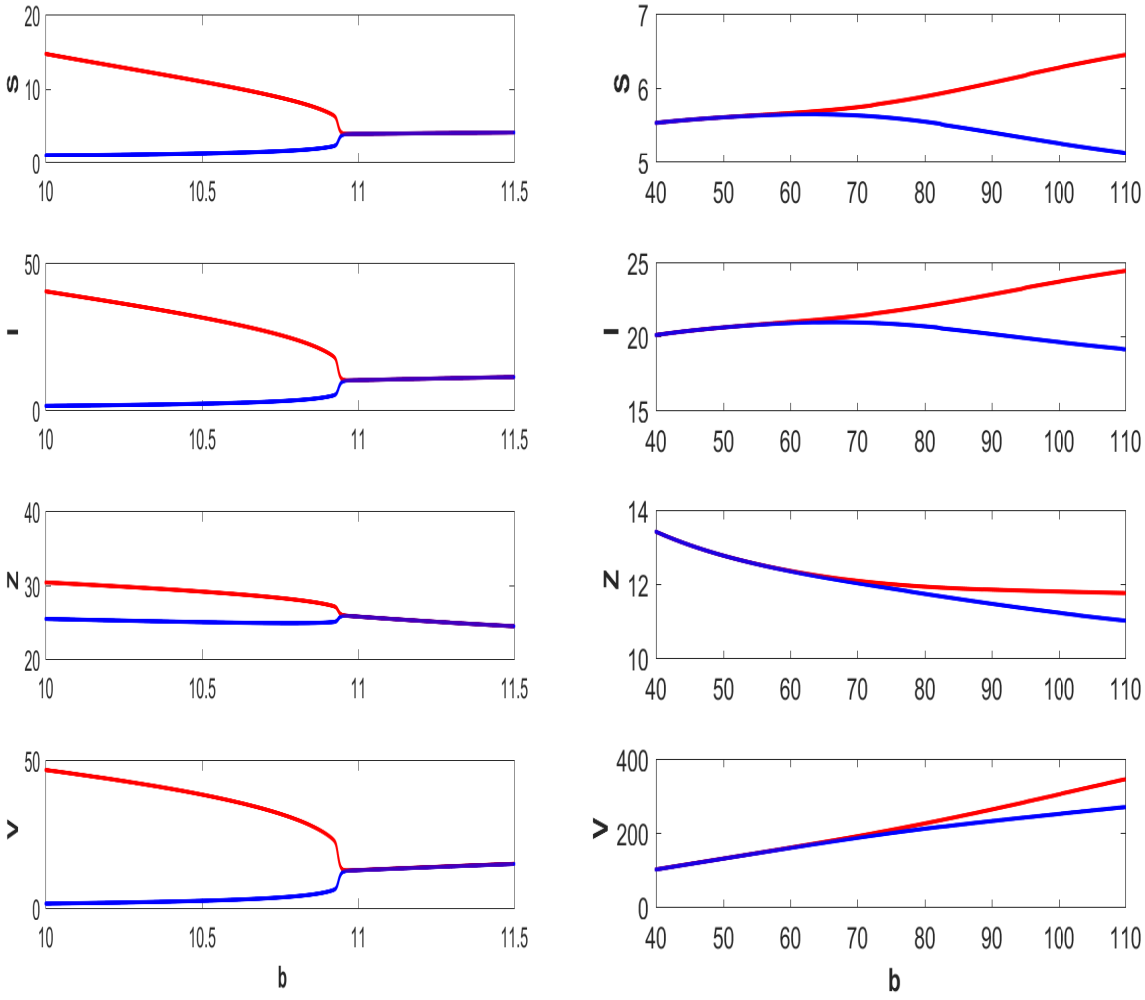

Fig. 8 Bifurcation diagram of the system (1) with respect to virus replication factor b. The two columns correspond to two very different ranges for this parameter value. Here, the maximum and minimum values of the oscillations are plotted in red and blue colors, respectively. Rest of the parameter values are the same as in Table 1.

maximum Lyapunov exponent with respect to β in Fig. 7, its positive values indicating the chaotic regime of the system.

Further, to visualize the effect of the virus replication factor on the system dynamics, we draw the bifurcation diagram by taking b as a bifurcation parameter, Fig. 8. Increasing the values of b, two critical values of b are found, $b_H^1 = 10.96$ and $b_H^2 = 65.15$, so that for $b < b_H^1$, limit cycle oscillations are observed, for $b_H^1 < b < b_H^2$, the system stabilizes, while for $b > b_H^2$ again persistent oscillations

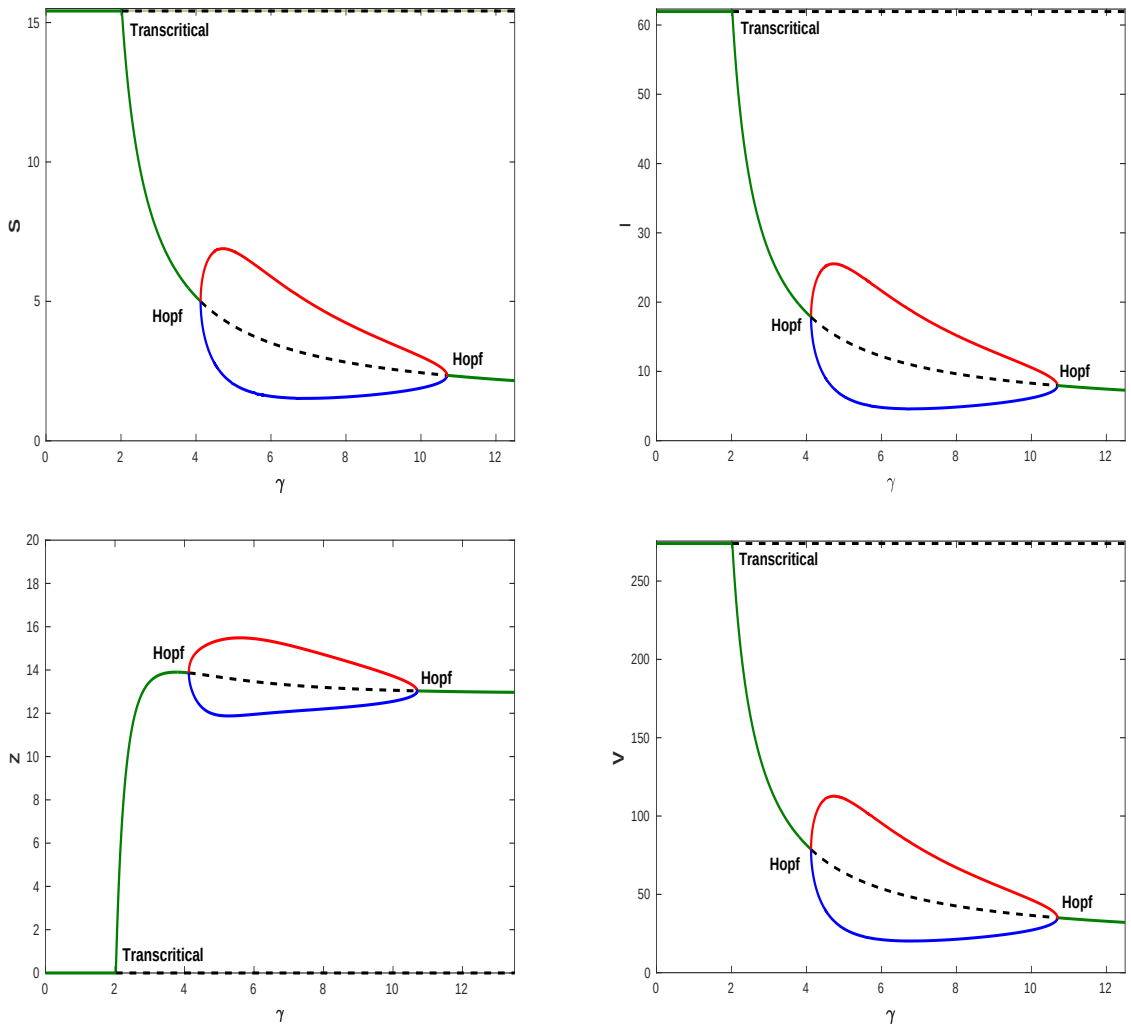

Fig. 9 Bifurcation diagram of the system (1) with respect to avoidance intensity, γ. Here, the maximum and minimum values of the oscillations are plotted in red and blue colors, respectively. Rest of the parameter values are the same as in Table 1.

appear. Furthermore, a bifurcation diagram in terms of the avoidance intensity γ is shown in Fig. 9. For low values of γ, the zooplankton-free equilibrium is stable, while on increasing it at the critical value $\gamma_T = 1.99$ the coexistence equilibrium emanates from the former. Further, there exist two critical values of γ, namely $\gamma_H^1 = 4.05$ and $\gamma_H^2 = 10.95$, such that at $\gamma = \gamma_H^1$, the system undergoes a supercritical Hopf-bifurcation and produces oscillations. Keeping on increasing the value of γ, the system undergoes a subcritical Hopf-bifurcation at $\gamma = \gamma_H^2$ after which it stabilizes again. Therefore, this ecosystem may show multiple stability switching depending on the values of virus replication factor and avoidance intensity. Note that in Fig. 9 we have chosen $\beta = 0.65$, which lies in the stable region of Fig. 6. Now,

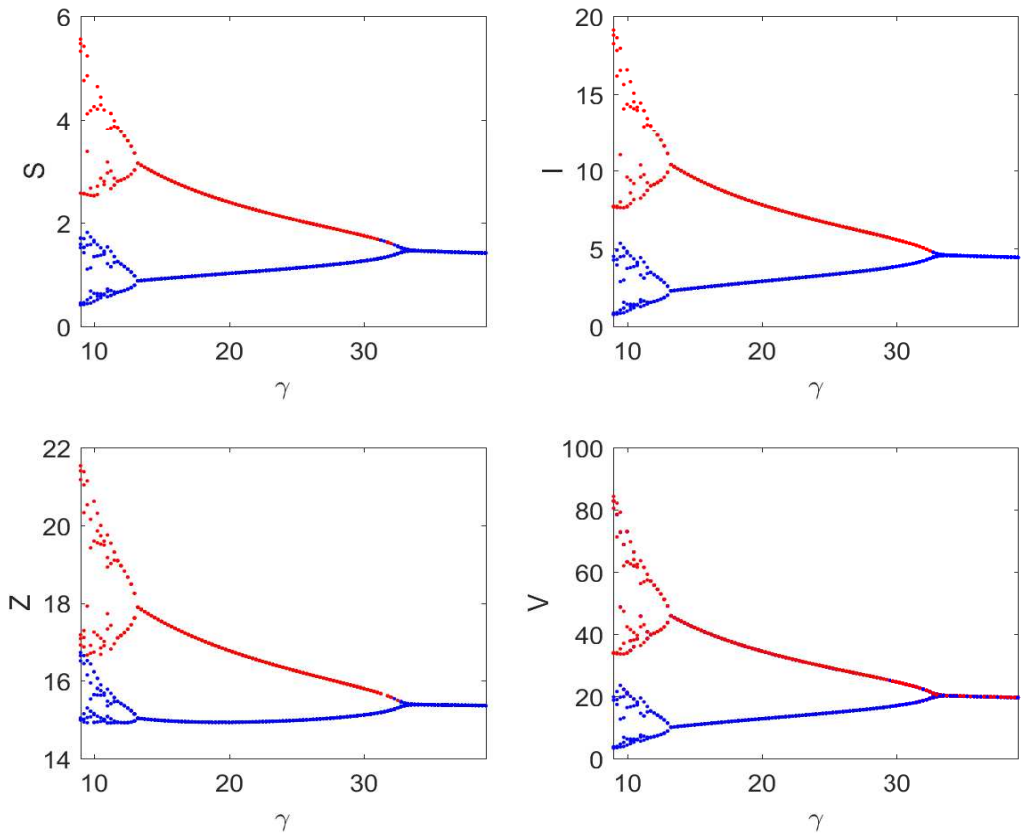

Fig. 10 Chaotic behavior of the system (1) with respect to intensity of avoidance (γ). Here, the maximum and minimum values of the oscillations are plotted in red and blue colors, respectively. Rest of the parameter values are the same as in Table 1 except $\beta = 0.62$.

we set $\beta = 0.62$, in the Hopf-region of Fig. 6, while keeping all the other parameters as in Table 1. We obtain that varying the avoidance parameter γ in the interval $[9, 39]$, Fig. 10, stable coexistence is achieved via a chaotic regime through period halving oscillations. The combined effect of the avoidance parameter γ and of the force of infection β are seen in Fig. 11, that portrays the different stability regions of the system (1). Here, blue, red, orange and green colors respectively represent the chaotic, period halving, limit cycle oscillation and stability domains. For higher values of the avoidance intensity, the ecosystem may show different stability behavior on increasing the force of infection. It goes possibly from chaos to period halving oscillations to limit cycle oscillations and finally to a stable focus. For intermediate values of β, the ecosystem experiences limit cycle oscillation to period doubling oscillation to chaotic behavior by increasing γ. Further simulations that are not reported indicate that for higher values of γ, chaos can be controlled and the system attains a stable focus. The stable equilibrium enters

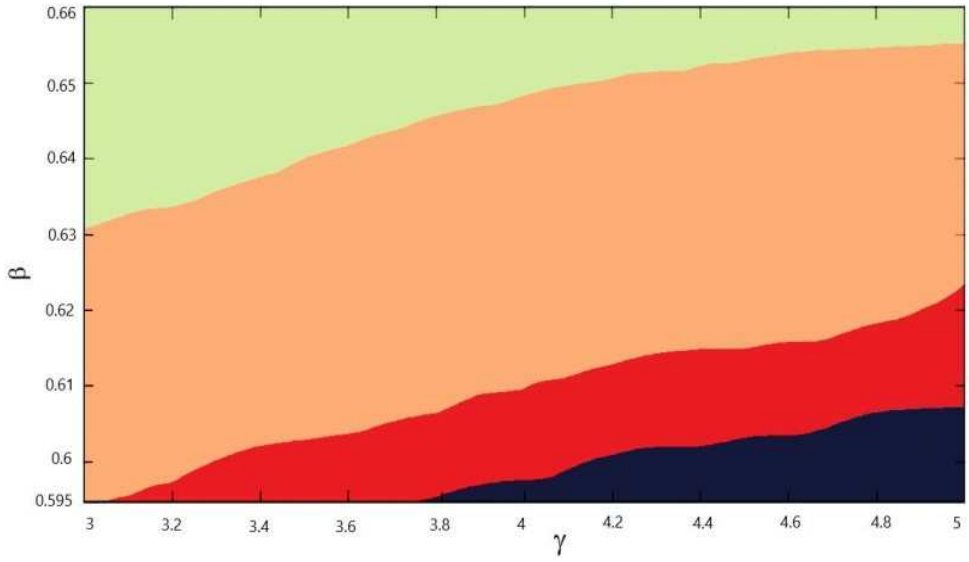

Fig. 11 Two-parameter bifurcation diagram as a function of γ and β. Regions in blue, red, orange and green colors represent chaotic, period halving, limit cycle and stable domains, respectively. Rest of the parameter values are the same as in Table 1.

into a chaotic regime through period doubling high-amplitude oscillations by increasing the values of K, i.e., increasing the nutrient supply, Fig. 12. This result is in line with the *paradox of enrichment* [61].

Next, we observe how the dynamics of the system changes if the susceptible phytoplankton feels the intraspecific pressure due to infected phytoplankton [39]. In such case, system (1) is reformulated as,

$$\begin{aligned}
\frac{dS}{dt} &= aS\left(1-\frac{S+I}{K}\right)-\frac{\alpha_1 SZ}{d_1+S}-\frac{\beta SV}{K_1+V},\\
\frac{dI}{dt} &= \frac{\beta SV}{K_1+V}-\frac{\alpha_2 IZ}{d_2+I+\gamma S}-\mu I,\\
\frac{dZ}{dt} &= \frac{\lambda_1\alpha_1 SZ}{d_1+S}-\frac{\lambda_2\alpha_2 IZ}{d_2+I+\gamma S}-\nu Z,\\
\frac{dV}{dt} &= b\mu I-\frac{\beta SV}{K_1+V}-\delta V.
\end{aligned} \tag{36}$$

The dynamics of (36) is investigated only by numerical simulations and compared with the findings of system (1). For low values of β, system (36) shows limit cycle oscillations but the oscillations vanish for increasing values of β, and for very high value of β, the zooplankton disappears from the system, Fig. 13(a). For low values of β, system (1) exhibits instead chaotic dynamics. Further, for low values of b, system (36) shows chaotic dynamics, but on increasing the values of b it switches to a stable focus

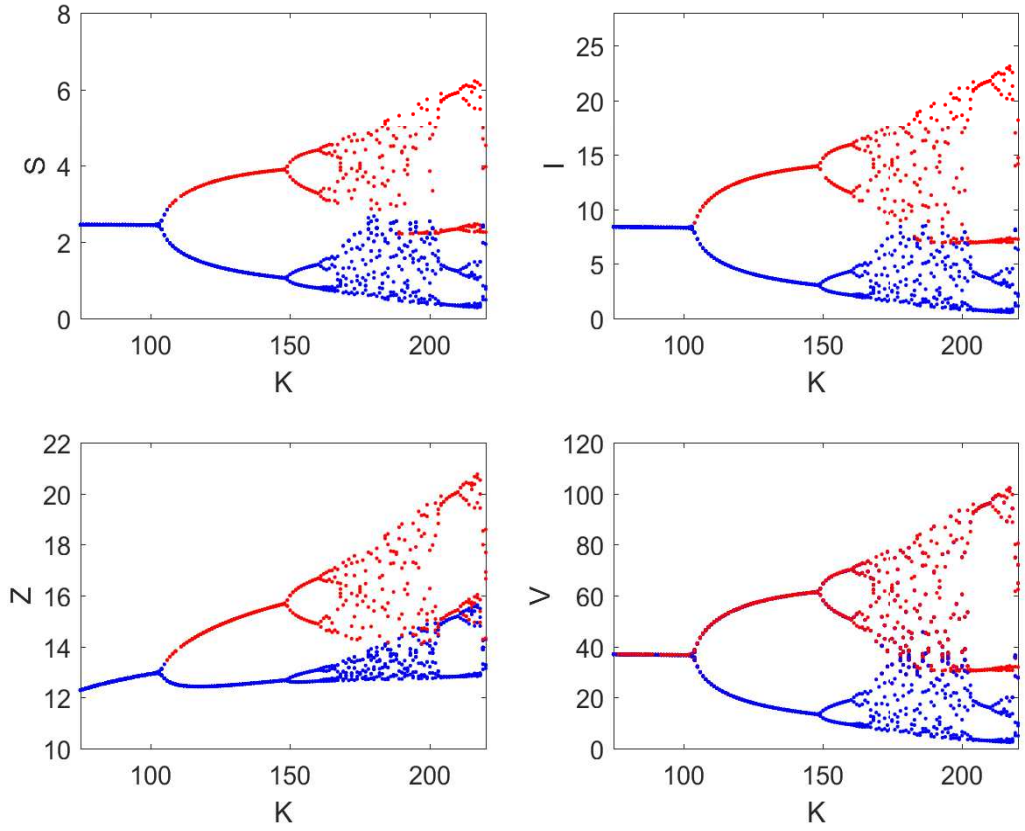

Fig. 12 Bifurcation diagram of the system (1) with respect to carrying capacity of the system (K). Here, the maximum and minimum values of the oscillations are plotted in red and blue colors, respectively. Rest of the parameter values are the same as in Table 1 except $\gamma = 10$.

through period halving bifurcation, Fig. 13(b). Moreover, for very high value of the parameter b, the zooplankton population does not survive in the system, Fig. 13(c). Recall that for very low and very high values of b, the system (1) shows limit cycle oscillations, and stable dynamics for moderate values of b. For low values of avoidance parameter, γ, system (36) shows extinction of zooplankton, and stable coexistence of all the populations after a threshold value of γ. Previously, we observed that the system (1) showed extinction of zooplankton for low values of γ, but on increasing the values of γ, the system experienced stability switches from stable to unstable to stable dynamics. We note that for low values of K, the zooplankton population becomes extinct from the system (this behavior is not observed for system (1)) but the coexistence equilibrium appears on increasing the values of K, see Fig. 13(e), and the system becomes chaotic for very large values of K, see Fig. 13(f).

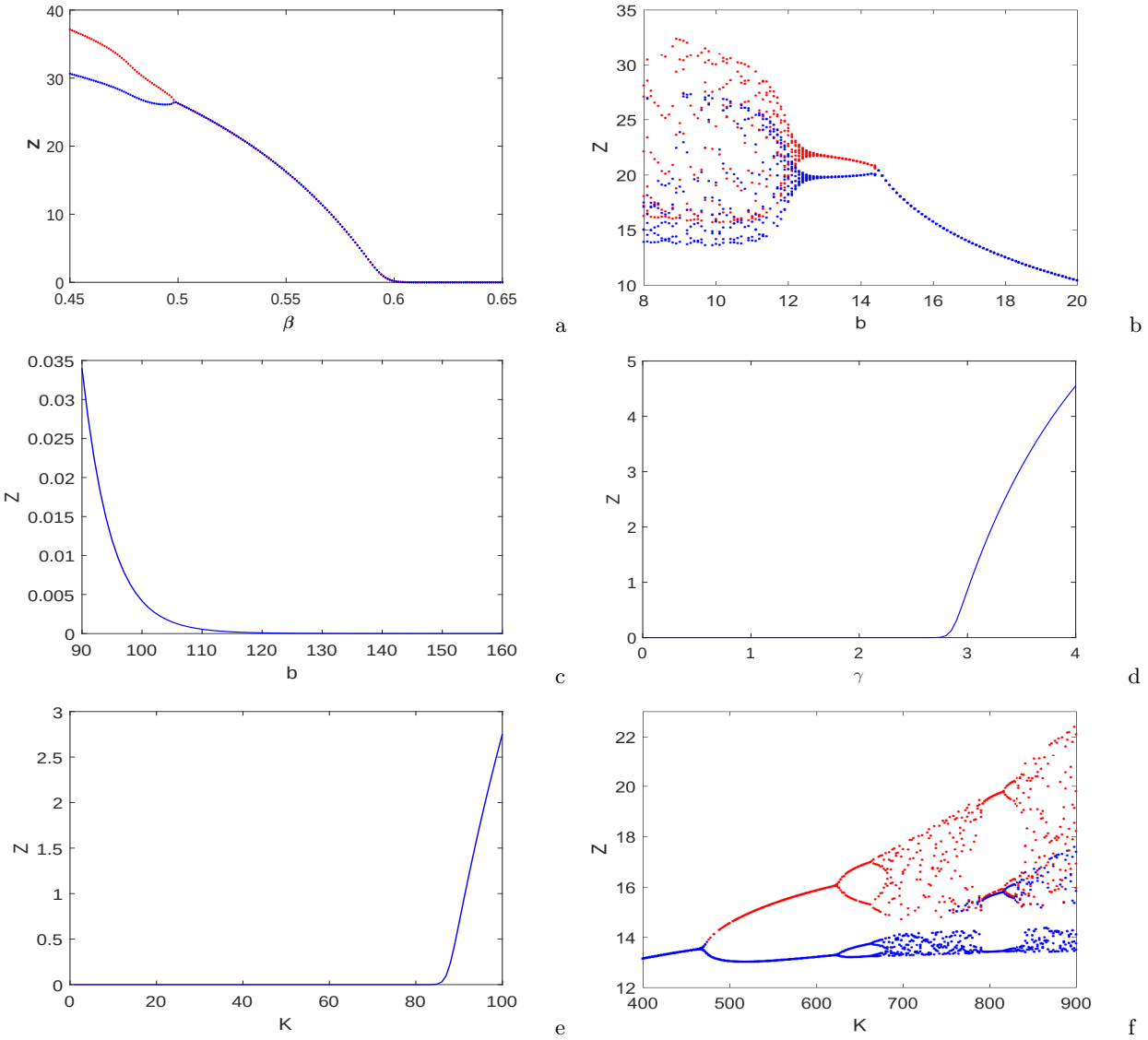

Fig. 13 System (36) shows (a) limit cycle oscillation for low values of β, (b) chaotic dynamics for low values of b, (c) extinction of zooplankton for very high value of b, (d) extinction of zooplankton for low values of γ but stable dynamics after a threshold value of γ, (e) extinction of zooplankton for low values of K, and (f) chaotic dynamics for very large values of K. Here, the maximum and minimum values of the oscillations are plotted in red and blue colors, respectively. Parameters are at the same value as in Table 1 except $\lambda_2 = 0.42$.

5 Conclusion and discussion

The interest in ecological studies of prey avoidance by a predator ranges from the details of individual feeding behavior to the implications for predator-prey dynamics. Some predators have the ability to discriminate between different types of prey and show avoidance to some specific prey population based on several known and unknown criteria [62]. In this paper, a mathematical model for the study

of the avoidance behavior of zooplankton on infected phytoplankton is proposed and its essential dynamical features are analyzed. The dynamics of free viruses is explicitly considered in the model. The partial rank correlation coefficient (PRCC) technique is performed to assess the sensitivity of the ecosystem with respect to the model parameters. The main parameters influencing the system behavior appear to be a, K, K_1, α_2, d_1, d_2, ν, δ, b and λ_2. They present positive correlations with the infected phytoplankton. Similarly, the parameters α_1, d_2, β, μ, δ, γ and λ_1 possess negative correlations with free viruses.

To identify the role of different parameters for the coexistence of all the populations, we use contour plots to represent the populations equilibrium values in terms of some important parameters: β, γ, μ, b, λ_1, λ_2, α_1, α_2, ν and δ. From these plots, the force of infection β, the virus replication factor b and the decay rate of free viruses δ appear to be important quantities to control the infection. To reduce disease prevalence in the phytoplankton, β and b should be reduced while δ should be fostered. On the other hand, the avoidance intensity γ fosters species coexistence. In the presence of viral infection, high intensity of zooplankton avoidance triggers the system chaotic behavior from a stable focus, due to nutrient enrichment. There is a minimum strength of the force of infection above which the infection becomes endemic in the system. Interestingly, increasing the infection rate the system switches from chaotic oscillations to a stable endemic equilibrium. Hence, the force of infection can control the chaotic behavior in this eco-epidemiological system. Further increasing the infection rate, the grazer zooplankton becomes extinct past a critical value of the force of infection. Increasing the virus replication factor values, the system stabilizes from persistent oscillations. If the virus replication factor exceeds a threshold value, the system becomes unstable again. Thus, the system shows multiple stability switching as a function of b, which therefore may play a crucial role in the system dynamics. A similar behavior for multiple stability switching is observed also in terms of the avoidance intensity, for which the system goes from a stable state to persistent oscillations via a supercritical Hopf bifurcation. Later on via another subcritical Hopf bifurcation, it stabilizes again. Our study suggests that the zooplankton's chance of extinction increases for lower values of the avoidance intensity. Interestingly, the avoidance parameter γ possesses a stabilizing role for the aquatic system by terminating the chaotic nature of the system. Thus, the avoidance parameter γ may be treated as a control parameter for the aquatic balance of the food web, indicating that the zooplankton avoidance of infected phytoplankton may significantly affect the ultimate ecosystem behavior.

Finally, we compare the dynamics of system (1) i.e., when infected phytoplankton do not compete for resources with the susceptible, with the system (36) i.e., when infected phytoplankton share resources with the susceptible ones. In the latter case, the system exhibits limit cycle oscillations (chaotic dynamics) for low values of force of infection (virus replication factor) while in the former case, the system shows chaotic dynamics (limit cycle oscillations) for low ranges of these two parameters. Moreover, in the second case, the system becomes zooplankton-free for higher values of the virus replication factor. The limit cycle oscillations also disappear for the second case on increasing the avoidance parameter, and interestingly the second model shows extinction of zooplankton for low values of the system carrying capacity.

The size of an organism affects virtually all aspects of its physiology and ecology [63]. The zooplankton body size gradually decreases during equilibrium condition in comparison to chaos [50]. Jørgensen et al. [64] showed that size combinations between phytoplankton and zooplankton are very crucial for the system's self-organization. The system cannot adapt to the gradual decrease of zooplankton size and as a result it moves from an equilibrium state to a chaotic condition. It is beneficial for low zooplankton populations to grow fast. If the fast growth continues the phytoplankton will be rapidly exhausted and in turn the zooplankton population will plunge, with the consequence that the system is led into violent oscillations and will ultimately attain chaos. This behavior however is not prevalent in many ecosystems, because they are self-organizing and self-adapting [65]. They tune themselves to a critical state [66] and show a high extent of self-organization based upon a hierarchy of feedback mechanisms. Among the many ways for which ecosystems can be self-adjusted, we have proposed and shown here that avoidance of virally infected phytoplankton by zooplankton, which reduces the zooplankton grazing, could be one of them and would help the system to recover from chaotic situation. These observations indicate that the avoidance of infected phytoplankton by zooplankton acts a bio-control by changing the state of chaos to order.

Acknowledgements

The authors are grateful to the anonymous referees for their careful reading, valuable comments and helpful suggestions, which have contributed to improve the presentation of this work significantly. Authors are grateful to Prof. Guido Badino, DBIOS, University of Turin, Italy for his valuable suggestions. The research work of Saswati Biswas is supported by Council of Scientific and Industrial Research, Government of India, New Delhi in the form of Senior Research Fellowship (Ref. No. 20/12/2015(ii)EU-V).

Pankaj Kumar Tiwari is thankful to University Grants Commissions, New Delhi, India for providing financial support in form of D. S. Kothari post-doctoral fellowship (No.F.4-2/2006 (BSR)/MA/17-18/0021). EV has been partially supported by the project "Metodi numerici e computazionali per le scienze applicate" of the Dipartimento di Matematica "Giuseppe Peano".

References

1. Vaulot, D.: Phytoplankton. In: Encyclopedia of Life Sciences. Macmillan Publishers Ltd. 1–7 (2001)
2. Evans, C., Pond, D.W., Wilson, W.H.: Changes in *Emiliania huxleyi* fatty acid profiles during infection with *E. huxleyi* virus 86: physiological and ecological implications. Aquat. Microb. Ecol. **55**, 219–228 (2009)
3. Gilg, I.C. et al.: Differential gene expression is tied to photochemical efficiency reduction in virally infected *Emiliania huxleyi*. Mar. Ecol. Prog. Ser. **555**, 13–27 (2016)
4. Malitsky, S. et al.: Viral infection of the marine alga *Emiliania huxleyi* triggers lipidome remodeling and induces the production of highly saturated triacylglycerol. New Phytol. **210(1)**, 88–96 (2016)
5. Rosenwasser, S. et al.: Rewiring host lipid metabolism by large viruses determines the fate of *Emiliania huxleyi*, a bloom-forming alga in the ocean. Plant Cell tpc-114 (2014)
6. Suzuki, T., Yasuo, S.: Virus infection and lipid rafts. Biol. Pharm. Bull. **29(8)**, 1538–1541 (2006)
7. Bratbak, G., Egge, J.K., Heldal, M.: Viral mortality of the marine alga *Emiliania huxleyi* (Haptophyceae) and termination of algal blooms. Mar. Ecol. Prog. Ser. 39–48 (1993)
8. Brussaard, C.P.D. et al.: Virus-like particles in a summer bloom of *Emiliania huxleyi* in the North Sea. Aquat. Microb. Ecol. **10**, 105–113 (1996)
9. Castberg, T. et al.: Microbial population dynamics and diversity during a bloom of the marine coccolithophorid *Emiliania huxleyi* (Haptophyta). Mar. Ecol. Prog. Ser. **221**, 39–46 (2001)
10. Nagasaki, K. et al.: Virus-like particles in *Heterosiginu akashiwo* (Raphidophyceae): a possible red-tide disintegration mechanism, Mar. Biol. **119(2)**, 307–312 (1994)
11. Jacquet, S. et al.: Flow cytometric analysis of an *Emiliana huxleyi* bloom terminated by viral infection. Aquat. Microb. Ecol. **27**, 111–124 (2002)
12. Costamagna, A. et al.: A model for the operations to render epidemic-free a hog farm infected by the Aujeszky disease. Appl. Math. Nonlinear Sci. **1(1)**, 207–228 (2016)
13. Venturino, E.: Ecoepidemiology: a more comprehensive view of population interactions. Math. Model. Nat. Phenom. **11(1)**, 49–90 (2016)
14. Samanta, S. et al.: Effect of enrichment on plankton dynamics where phytoplankton can be infected from free viruses. Nonlinear Studies **20(2)**, 223–236 (2013)
15. Bairagi, N. et al.: Virus replication factor may be a controlling agent for obtaining disease-free system in a multi-species eco-epidemiological system. J. Biol. Syst. **13(3)**, 245–259 (2005)
16. Evans, C., Wilson, W.H.: Preferential grazing of Oxyrrhis marina on virus infected *Emiliania huxleyi*. Limnol. Oceanogr. **53**, 2035–2040 (2008)

17. Vermont, A. et al.: Virus infection of *Emiliania huxleyi* deters grazing by the copepod *Acartia tonsa*. J. Plankton Res. **38(5)**, 1194–1205 (2016)
18. Townsend, D.W. et al.: Blooms of the coccolithophore *Emiliania huxleyi* with respect to hydrography in the Gulf of Maine. Cont. Shelf Res. **14**, 979–1000 (1994)
19. Wilson, W.H. et al.: Isolation of viruses responsible for the demise of an *Emiliania huxleyi* bloom in the English Channel. J. Mar. Biol. Assoc. U.K. **82(3)**, 369–377 (2002)
20. Evans, C.: The influence of marine viruses on the production of dimethyl sulphide (DMS) and related compounds from *Emiliania huxleyi*. PhD Thesis, University of East Anglia (2005)
21. Evans, C. et al.: Viral infection of *Emiliania huxleyi* (Prymnesiophyceae) leads to elevated production of reactive oxygen species. J. Phycol. **42**, 1040–1047 (2006)
22. Poulet, S.A., Ouellet, G.: The role of amino acids in the chemosensory swarming and feeding of marine copepods. J. Plankton Res. **4**, 341–361 (1982)
23. Gill, C.W., Poulet, S.A.: Responses of copepods to dissolved free amino acids. Mar. Ecol. Prog. Ser. **43**, 269–276 (1988)
24. Demott, W.R., Watson, M.D.: Remote detection of algae by copepods: responses to algal size, odors and motility. J. Plankton Res. **13**, 1203–1222 (1991)
25. Steinke, M., Stefels, J., Stamhuis, E.: Dimethyl sulfide triggers search behavior in copepods. Limnol. Oceanogr. **51**, 1925–1930 (2006)
26. Floge, S.A.: Virus infections of eukaryotic marine microbes, Electronic Theses and Dissertations. The University of Maine (2014)
27. Evans, C. et al.: The relative sinificance of viral lysis and microzooplankton grazing as pathways of dimethylsulfoniopropionate (DMSP) cleavage: an *Emiliania huxleyi* culture study. Limnol. Oceanogr. **52**, 1036–1045 (2007)
28. Predators in the Plankton, Available at `http://oceans.mit.edu/news/featured-stories/predators-in-the-plankton.html`
29. Mukherjee, D.: Persistence in a prey-predator system with disease in the prey. J. Biol. Syst. **11(01)**, 101–112 (2003)
30. Venturino, E.: Epidemics in predator-prey models: disease in the prey, In: Arino, O., Axelrod,D., Kimmel,M., Langlais,M. (Eds.), Mathematical Population Dynamics: Analysis of Heterogeneity, **1**, 381–393 (1995)
31. Chattopadhyay, J., Arino, O.: A predator-prey model with disease in the prey. Nonlinear Analysis **36**, 747–766 (1999)
32. Hethcote, H.W. et al.: A predator-prey model with infected prey. Theor. Popul. Biol. **66(3)**, 259–268 (2004)
33. Beretta, E., Kuang, Y.: Modeling and analysis of a marine bacteriophage infection. Math. Biosci. **149**, 57–76 (1998)
34. Siekmann, I., Malchow, H., Venturino, E.: An extension of the Beretta-Kuang model of viral diseases. Math. Biosci. Eng. **5**, 549–565 (2008)
35. Hilker, F.M. et al.: Oscillations and waves in a virally infected plankton system Part II: Transition from lysogeny to lysis. Ecol. Compl. **3**, 200–208 (2006)

36. Bhattacharyya, S., Bhattacharya, D.K.: Pest control through viral disease: mathematical modeling and analysis. J. Theor. Biol. **238(1)**, 177–197 (2006)
37. Beltrami, E., Carroll, T.O.: Modeling the role of viral disease in recurrent phytoplankton blooms. J. Math. Biol. **32**, 857–863 (1994)
38. Gakkhar, S., Negi, K.: A mathematical model for viral infection in toxin producing phytoplankton and zooplankton system. Appl. Math. Comp. **179**, 301–313 (2006)
39. Chattopadhyay, J., Pal, S.: Viral infectionon phytoplankton-zooplankton system: a mathematical model. Ecol. Model. **151**, 15–28 (2002)
40. Rhodes, C., Truscott, J., Martin, A.: Viral infection as a regulator of oceanic phytoplankton populations. J. Mar. Syst. **74**, 216–226 (2008)
41. Singh, B.K., Chattopadhyay, J., Sinha, S.: The role of virus infection in a simple phytoplankton-zooplankton system. J. Theor. Biol. **231**, 153–166 (2004)
42. Rhodes, C.J., Martin, A.P.: The influence of viral infection on a plankton ecosystem undergoing nutrient enrichment. J. Theor. Biol. **265(3)**, 225–237 (2010)
43. May, R.M.: Chaos and the dynamics of biological populations. Proc. R. Soc. Lond. **413**, 27–44 (1987)
44. Godfray, H.C.J., Grenfell, B.T.: The continuing quest for chaos. Trends Ecol. Evol. **8**, 43–44 (1993)
45. Hastings, A. et al.: Chaos in ecology: is mother nature a strange attractor? Annu. Rev. Ecol. Syst. **24**, 1–33 (1993)
46. Perry, J.N., Woiwod, I.P., Hanski, I.: Using response-surface methodology to detect chaos in ecological time series. Oikos **68**, 329–339 (1993)
47. Jørgensen, S.E.: The growth rate of zooplankton at the edge of chaos: ecological models. J. Theor. Biol. **175**, 13–21 (1995)
48. Hastings, A., Powell, T.: Chaos in three-species food chain. Ecology **72**, 896–903 (1991)
49. Chattopadhyay, J., Sarkar, R.R.: Chaos to order: preliminary experiments with a population dynamics models of three trophic levels. Ecol. Model. **163**, 45–50 (2003)
50. Peters, R.H.: The ecological implications of body size. Cambridge University Press, Cambridge (1983)
51. Mandal, S. et al.: Order to chaos and vice versa in an aquatic ecosystem. Ecol. Model. **197**, 498–504 (2006)
52. Chakraborty, S. et al.: The role of avoidance by zooplankton for survival and dominance of toxic phytoplankton. Ecol. Compl. **11**, 144–153 (2012)
53. Holmes, J.C., Bethel, W.M.: Modification of intermediate host behavior by parasites, In: Canning, E.V., Wright, C.A. (Eds.), Behavioral Aspects of Parasite Transmission. Suppl. I to Zool. f. Linnean Soc. **51**, 123–149 (1972)
54. Lafferty, K.D.: Foraging on prey that are modified by parasites. Am. Nat. **140**, 854–867 (1992)
55. Hamilton, W.D., Axelrod, R., Tanese, R.: Sexual reproduction as an adaptation to resist parasite: a review. Proc. Natl Acad. Sci. USA **87**, 3566–3573 (1990)
56. Uhlig, G., Sahling, G.: Long-term studies on Noctilucascintillans in the German bight. Neth. J. Sea Res. **25**, 101–112 (1992)
57. Lakshmikantham, V., Leela, S., Martynyuk, A.A.: Stability analysis of nonlinear systems. Marcel Dekker, Inc. New York/Basel (1989)

671 58. Smith, H.L.: The Rosenzweig-Macarthur predator-prey model. https://math.la.asu.edu/halsmith/
672 Rosenzweig.pdf
673 59. Li, Y., Muldowney, J.S.: On Bendixson's criterion, J. Diff. Eqn. **106**, 27–39 (1993)
674 60. Marino, S. et al.: A methodology for performing global uncertainty and sensitivity analysis in systems
675 biology. J. Theor. Biol. **254(1)**, 178–196 (2008)
676 61. Rosenzweig, M.L.: Paradox of enrichment: destabilization of exploitation ecosystems in ecological time.
677 Science **171**, 385 (1971)
678 62. Linhart, S.B. et al.: Avoidance of prey by captive coyotes punished with electric shock. In: Proceedings of
679 the Vertebrate Pest Conference **7**, 302–330 (1976)
680 63. Lebedeva, L.P.: A model of the latitudinal distribution of the numbers of species of phytoplankton in the
681 sea. J. Cons. Int. Explor. Mer. **34**, 341–350 (1972)
682 64. Jørgensen, S.E. et al.: Improved calibration of a eutrophication model by use of the size variation due to
683 succession. Ecol. Model. **153**, 269–277 (2002)
684 65. Odum, H.T.: Self organization, transformity, and information. Science **242**, 1132–1139 (1988)
685 66. Kauffman, S.A.: Anti-chaos and adaptation. Sci. Am. **265(2)**, 78–84 (1991)